temperature (A). The appearance of translucent dots behind the sublimation front suggested the onset of physical collapse (T_c, B). Further heating of the frozen solution induced intensive loss of the structure in the region (C). The frozen solutions containing PVP 29,000 and dextran 35,000 (50 mg/mL each) also showed an ordered dried region at the lower temperature (D). The emergence of translucent dots, which indicates the onset of collapse, was rather unclear in the phase-separating frozen polymer solution (E). The ice sublimation advanced, leaving a reticulate dried region for several degrees, before significant deterioration of the solid structure (F). The temperatures of the translucent dot emergence and transition to the large structural change were assigned as T_{c1} and T_{c2} in this study.

Figure 3 shows the relationship between the polymer compositions and the T_cs of the frozen solutions obtained by the FDM analysis. The thermal transition temperatures (T'_g) are also included in the figure for comparison. Each polymer used in the study showed an apparent collapse at a temperature(PVP 10,000: −21.7°C, PVP 29,000: −19.4°C, dextran 1060: −19.1°C, dextran 35,000: −10.3°C)

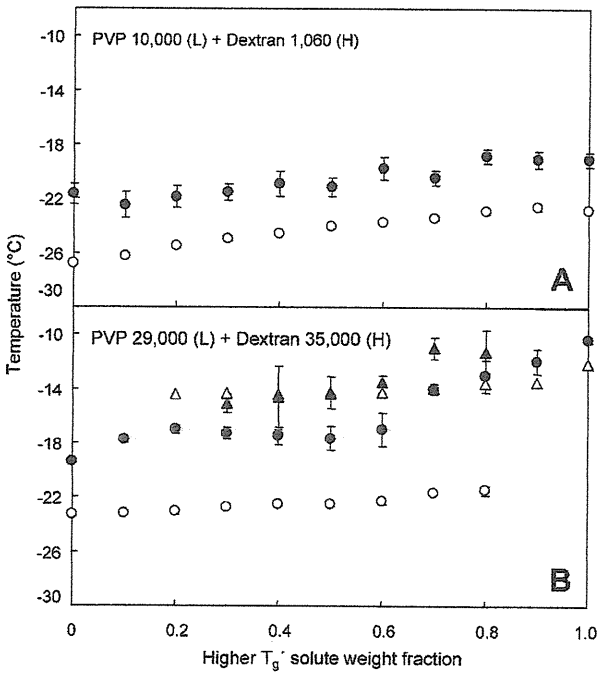

Figure 3. Collapse temperatures of frozen solutions containing PVP 10,000 and dextran 1060 (A) and PVP 29,000 and dextran 35,000 (B) (100 mg/mL total) obtained by freeze-drying microscopy. Each symbol denotes the average ± SD ($n = 3$) of the collapse onset temperature (T_c, T_{c1}: ●) and the second collapse temperature (T_{c2}: ▲). Thermal transition temperatures of the corresponding frozen solutions (T'_g, T'_{g1}: ○, T'_{g2}: Δ) are included for comparison.

several degrees (2.9–5.1°C) higher than the corresponding T'_{g1} obtained by thermal analysis. The phase-separating frozen PVP 29,000 and dextran 35,000 solutions showed collapse onset (T_{c1}) above the T'_g. Some frozen solutions also showed transition to the severe structural change (T_{c2}). There were large shifts in the collapse temperatures at certain (between 60 and 70 mg/mL) dextran concentration ratios.

Experimental Freeze-Drying

Freeze-drying of the polymer mixture solutions at different shelf temperatures (−32 to −12°C) during the primary drying segment resulted in collapsed or cake-structure solids (Fig. 4). The miscible solute combinations (dextran 1060 and PVP 10,000 or dextran 35,000) showed significantly different solid structures depending on the shelf temperatures below (cake-structure) and above (collapsed solid) their composition-dependent T'_gs during primary drying. No difference was observed in the appearance of the solids freeze-dried at several positions on the shelves. The slower primary drying process carried out at higher chamber pressures kept the difference between the designated shelf temperatures and those of products within 2°C (data not shown).[5] The usual primary drying process at reduced pressures should significantly lower the product temperature by faster ice sublimation. Limitations with regard to controlling the pressure of the system made it difficult to appropriately keep the product temperatures above −12°C in this study.

The phase-separating polymer combination (PVP 29,000 and dextran 35,000) also retained the cake structure in freeze-drying at temperatures below both of the T'_gs (<−24°C). Freeze-drying of the polymer combinations at temperatures between the two T'_gs (−22 and −14°C) resulted in apparently different solid structures depending on the main polymer component in the initial solutions. Figure 5 shows the typical appearance of the lyophilized solids containing PVP 29,000 and dextran 35,000 obtained at a primary drying temperature (−16°C). The solutions containing more than 50 mg/mL dextran 35,000 were dried as cake-structure solids without apparent volume change. Some of the cake-structure polymer mixture solids (e.g., 50–70 mg/mL dextran 35,000) freeze-dried at −20 to −14°C showed a coarse surface texture compared to those dried at −32°C (data not shown). In contrast, the mixtures containing a higher concentration ratio of PVP 29,000 lost their cylindrical structure during primary drying between −22 and −14°C. Colyophilization with NaSCN induced overall collapse at temperatures slightly higher than the single T'_g of each mixture.

DOI 10.1002/jps

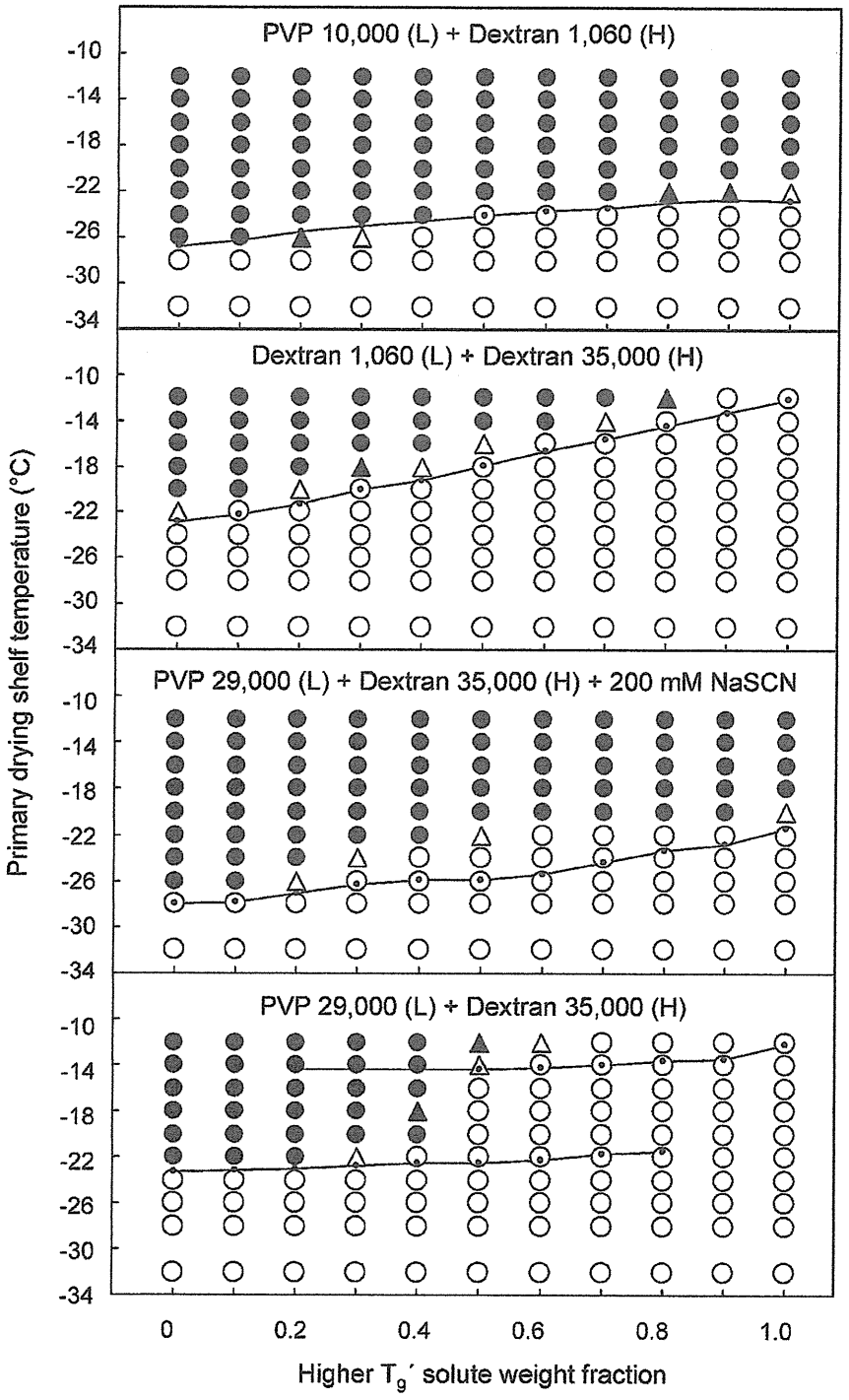

Figure 4. Structure of polymer mixture solids freeze-dried at different temperatures. The initial aqueous solution contained solutes that have lower (L) and higher (H) intrinsic transition temperatures (T_g'). The symbols denote a cake-structure solid (○), slightly shrunk cake (Δ), shrunk cake (▲), and collapsed solid (●). Thermal transition temperatures of the corresponding frozen solutions (T_g', T_{g1}', T_{g2}') are plotted as small dots and lines.

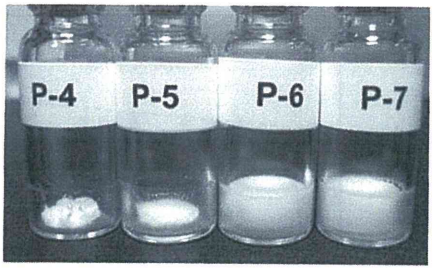

(mg/ml)				
PVP 29,000	70	60	50	40
Dextran 35,000	30	40	50	60

Figure 5. Images of freeze-dried solids containing PVP 29,000 and dextran 35,000 obtained at a shelf temperature (−16°C) during the primary drying process.

Scanning Electron Microscopy Analysis of Freeze-Dried Solids

Figure 6 shows SEM images of the polymer solids freeze-dried at different temperatures. Freeze-drying of solutions containing PVP 29,000, dextran 35,000, or their mixture at temperatures below all the T'_gs (−32°C) resulted in microporous cake-structure solids with a fine-edged local structure. Primary drying at the higher shelf temperature (−16°C) did not affect the morphology of the cake-structure dextran 35,000 solid. In contrast, the high primary drying temperature induced both physical collapse and microscopic structure changes of PVP 29,000. The polymer mixture dried at −16°C showed a round-shaped domain structure, although the cylindrical solid retained the volume of the original solution, which strongly suggested microscopic collapse in the primary drying at temperatures between the two T'_gs. No apparent difference in the amount of residual water was observed in these polymer solids (<1% (w/w), data not shown).

DISCUSSION

The results indicated the relevance of characterizing frozen solutions and freeze-dried solids in the formulation and process development of multicomponent lyophilized pharmaceuticals. Availability of the various molecular weight polymers and their apparent thermal transitions made the PVP and dextran mixture an excellent model to study their miscibility in frozen solutions. Thermal analysis of frozen solutions showed different miscibilities of PVP and dextran depending on their molecular size and concentration ratios.[18–21] The large PVP and dextran molecules were freeze-concentrated into different phases that contain specific ratios of a major solute and a minor counterpart component, as has been reported previously in aqueous two-layer systems.[21,24] The absence of apparent clouding before ice formation and the two T'_gs also observed in freezing a lower concentration initial solution (10 mg/mL each) indicated that the increased solute concentrations due to ice growth, rather than the lower

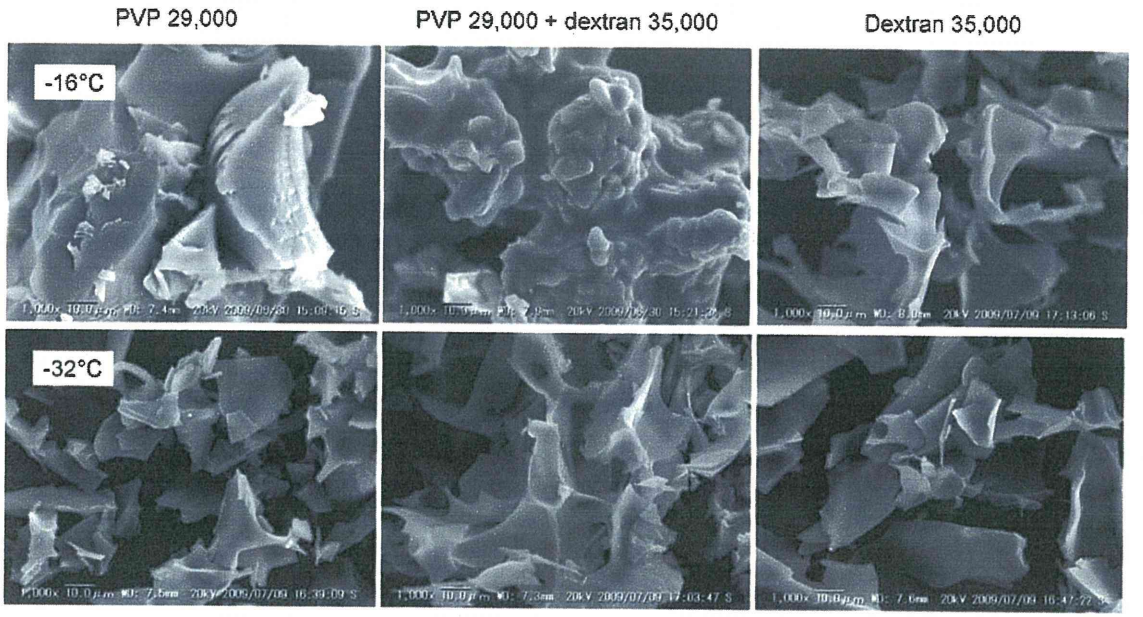

Figure 6. Scanning electron micrographs of solids containing PVP 29,000, dextran 35,000, and their mixture (total 100 mg/mL) obtained by freeze-drying at two primary drying temperatures (−16 and −32°C).

DOI 10.1002/jps

temperatures, were the primary cause of the immiscibility in frozen solutions.[22] Polymers dominant in one of the components may remain in the same concentrated phase. Thermal analysis also showed mixing of smaller PVP and dextran molecules in the frozen solutions. Reported aqueous two-layer formation in response to various polymer combinations, including proteins and polymer excipients, suggests possible component immiscibility in their frozen solutions caused by the thermodynamically unfavorable interactions and excess concentrations.[25,26] The various levels of solute miscibility in the frozen solutions should affect the quality of lyophilized pharmaceutical formulations in various ways.[19] Limited mobility of solute molecules during appropriate freeze-drying process would retain their varied miscibility in the frozen solutions.[32]

The miscible and immiscible solute combinations showed different propensities to collapse during experimental freeze-drying at various shelf temperatures. Maintaining the frozen solution at temperatures slightly lower than the T_c (or T'_g) during the primary drying, which allows a higher ice sublimation speed and a rigid freeze-concentrated phase, is a widely accepted means of obtaining cake-structure amorphous solids from single-solute or miscible multisolute aqueous frozen solutions.[1,5,6,8] The collapse onset temperatures (T_cs) of the frozen miscible polymer solutions were observed at temperatures several degrees higher than the corresponding T'_gs.[12,16,30] The high solute concentrations that increase the solid density and technical difficulties in distinguishing collapse onset in the FDM analysis may partially explain the large difference between the T'_gs and T_cs. Various other factors (e.g., apparatus, scanning speed) also affect the T_cs.[16]

The phase-separating larger polymer mixtures showed more complicated collapse phenomena that depend on the component composition. Lyophilization without overall collapse is one of the prerequisites for the multiphased formulations containing highly potent and structurally fragile active ingredients and/or delivery carriers. The schematic relationship between the solute composition (PVP 29,000 and dextran 35,000), the transition temperatures (T'_g), and their physical integrity during lyophilization at various primary drying temperatures is shown in Figure 7. The frozen polymer solutions showed two T'_gs at widely varied concentration ratios. It is reasonable to suppose that rigid amorphous freeze-concentrated phases retain their local morphology and overall cake structure following primary drying below all the T'_gs. In contrast, the uniformly lower viscosities of the separated phases at the product temperatures above all the T'_gs should induce a significant collapse of materials during the primary drying process.

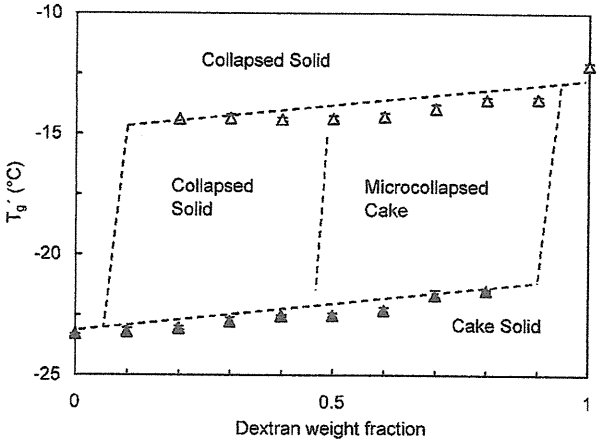

Figure 7. Schematic relationship between the component composition, transition temperature (T'_g), and structural integrity of freeze-dried phase-separating systems containing PVP 29,000 and dextran 35,000.

The occurrence of microcollapse (microscopically disordered cylindrical cake-structure solids) in the primary drying of dextran-rich frozen solutions at shelf temperatures between the two T'_gs (i.e., microcollapsing window) should be of particular interest with regard to freeze-drying of the phase-separating systems. Different local viscosities of the separated polymer phases in this temperature range should induce microcollapse or overall collapse depending on the quantitative and dynamic balance of the phases at the drying interface. The mechanism of the microcollapse phenomena observed in multiphased polymer systems should be different from that of the partial collapse that occurs during freeze-drying of some single-solute and miscible multisolute systems in their intermediate viscosity state near the single T'_gs, although both can induce locally altered structures. The phase-separating polymer system showed spreading of the reticulate microcollapsed dried region following collapse onset (T_{c1}) for wide temperature ranges (1.8–3.5°C in the PVP 29,000 and dextran 35,000 mixture) before the severe structural change (T_{c2}) in the FDM heating scan. The margin between the two temperatures should vary depending on the T'_gs of the particular system. It is plausible that the local structural change starts at temperatures lower than the observed collapse onset (T_{c1}). In contrast, the single-solute and miscible multipolymer systems showed intense structural change immediately after the collapse onset.

The polymers that form a concentrated higher T'_g phase should contribute to the formation of microcollapsed solids in a manner similar to that of crystallizing solutes.[28] Quantitative advantage of the dextran-rich phase should allow the microscopic structure change of the higher fluidity PVP-rich

phase on the rigid microporous cake-structure matrix during primary drying between the two T'_gs. In contrast, insufficient physical intensity of a system dominant in PVP should induce the overall structural collapse from the ice sublimation front. Changes in this balance may explain the large T_c shift observed at a particular dextran concentration ratio. Limited viscosity changes in the coexisting freeze-concentrated phases between the two T'_gs would explain the similar structure of the particular composition solids lyophilized at the temperature range. Decreasing viscosities of the matrix above the higher T'_g (amorphous solute) or T_{eu} (crystalline solute) should lead to overall collapse during the primary drying process.

The phase-separating multisolute frozen solutions provide several options in the formulation and process design that affect the efficiency and robustness of the lyophilization cycle, as well as the product quality. Primary drying at temperatures lower than the T'_gs of all phases is the conventional method for ensuring better product quality at the expense of a longer segment time. Choosing the formulation and process parameters that results in amorphous microcollapsed solids is a promising strategy for achieving faster ice sublimation and cake-structure appearance. Some lower T'_g pharmaceutically active ingredients could be lyophilized in the microcollapsed state by adding a phase-separating high-T'_g matrix polymer (e.g., dextran). The microcollapse, however, can affect the quality of pharmaceutical formulations either directly (e.g., damage higher order structures of biomacromolecules) or indirectly (e.g., reduced storage stability by higher residual water contents) as reported in the collapse of whole systems.[5,33] The effects of microcollapse and their acceptability are interesting topics that require further study.

Understanding the complex physical behavior of phase-separating frozen solutions is relevant for the formulation and process optimization of various lyophilized pharmaceuticals.[13–15] Some polymer excipients (e.g., PVP) protect proteins directly (e.g., reduce freezing-induced oligomer dissociation[34]) and indirectly (e.g., reduce chemical degradation by raising glass transition temperature of colyophilized disaccharide-based solids[1]) during the process and storage. Further studies that clarify phase behavior of the complex systems are required for rational design of the polymer-containing protein formulations since many frozen protein solutions show only unclear T'_g transition in thermal analysis. Similar approach would be applicable to some freeze-dried suspension formulations that form concentrated medium and particle phases in frozen solutions. Monitoring of various changes during freeze-drying by appropriate process analytical technology (PAT) tools (e.g., measurement of residual ice by Raman spectroscopy) should also assist in the implementation of robust freeze-drying cycles.[35–38]

ACKNOWLEDGMENTS

This work was partially supported by the Japan Human Sciences Foundation (Research on Publicly Essential Drugs and Medical Devices, KHB1006), the Japan Society for the Promotion of Sciences (Scientific Research C, #19590044), and the Promotion and Mutual Aid Corporation for Private Schools of Japan (Science Research Promotion Fund).

REFERENCES

1. Nail SL, Jiang S, Chongprasert S, Knopp SA. 2002. Fundamentals of freeze-drying. Pharm Biotechnol 14:281–360.
2. Tang X, Pikal MJ. 2004. Design of freeze-drying processes for pharmaceuticals: Practical advice. Pharm Res 21:191–200.
3. Carpenter JF, Chang BS, Garzon-Rodriguez W, Randolph TW. 2002. Rational design of stable lyophilized protein formulations: Theory and practice. Pharm Biotechnol 13:109–133.
4. Mehnert W, Mäder K. 2001. Solid lipid nanoparticles: Production, characterization and applications. Adv Drug Deliv Rev 47:165–196.
5. Chang BS, Patro SY. 2004. Freeze-drying process development for protein pharmaceuticals. In: Costantino HR, Pikal MJ, editors. Lyophilization of biopharmaceuticals. Arlington: American Association of Pharmaceutical Scientists, pp 113–138.
6. Akers MJVV, Stickelmeyer M. 2002. Formulation development of protein dosage forms. Pharm Biotechnol 14:47–127.
7. Kuu WY, Hardwick LM, Akers MJ. 2005. Correlation of laboratory and production freeze drying cycles. Int J Pharm 302: 56–67.
8. Franks F. 1990. Freeze-drying: From empiricism to predictability. Cryo-Letters 11:93–110.
9. Luyet BJ. 1939. The devitrification temperatures of solutions of a carbohydrate series. J Phys Chem 43:881–885.
10. MacKenzie AP. 1971. Non-equilibrium freezing behaviour of aqueous systems. Phil Trans R Soc Lond B 278:167–189.
11. Lee MK, Kim MY, Kim S, Lee J. 2009. Cryoprotectants for freeze drying of drug nano-suspensions: Effect of freezing rate. J Pharm Sci 98:4808–4817.
12. Pikal MJ, Shah S. 1990. The collapse temperature in freeze drying: Dependence on measurement methodology and rate of water removal from glassy phase. Int J Pharm 62:165–186.
13. Kasraian K, Spitznagel TM, Juneau JA, Yim K. 1998. Characterization of the sucrose/glycine/water system by differential scanning calorimetry and freeze-drying microscopy. Pharm Dev Technol 3:233–239.
14. Adams GDJ, Ramsay JR. 1996. Optimizing the lyophilization cycle and the consequences of collapse on the pharmaceutical acceptability of Erwinia L-asparaginase. J Pharm Sci 85:1301–1305.
15. MacKenzie AP. 1964. Apparatus for microscopic observations during freeze-drying (AFBR freeze-drying microscope model 2). Biodynamica 9:213–222.
16. Meister E, Gieseler H. 2009. Freeze-dry microscopy of protein/sugar mixtures: Drying behavior, interpretation of collapse temperatures and a comparison to corresponding glass transition data. J Pharm Sci 98:3072–3087.

DOI 10.1002/jps

17. Shamblin SL, Taylor LS, Zografi G. 1998. Mixing behavior of colyophilized binary systems. J Pharm Sci 87:694–701.
18. Heller MC, Carpenter JF, Randolph TW. 1996. Effects of phase separating systems on lyophilized hemoglobin. J Pharm Sci 85:1358–1362.
19. Randolph TW. 1997. Phase separation of excipients during lyophilization: Effects on protein stability. J Pharm Sci 86: 1198–1203.
20. Izutsu K, Yoshioka S, Kojima S, Randolph TW, Carpenter JF. 1996. Effect of sugars and polymers on crystallization of poly(-ethylene glycol) in frozen solutions: Phase separation between incompatible polymers. Pharm Res 13:1393–1400.
21. Izutsu K, Aoyagi N, Kojima S. 2005. Effect of polymer size and cosolutes on phase separation of poly(vinylpyrrolidone) (PVP) and dextran in frozen solutions. J Pharm Sci 94:709–717.
22. Izutsu K, Heller M, Randolph TW, Carpenter JF. 1998. Effect of salts and sugars on phase separation of polyvinylpyrrolidone-dextran solutions induced by freeze-concentration. J Chem Soc Faraday Trans 94:411–418.
23. Gustafsson A, Wennerstorm H, Tjerneld F. 1986. The nature of phase separation in aqueous two-polymer systems. Polymer 27:1768–1770.
24. Albertsson PA. 1970. Partition of cell particles and macromolecules in polymer two-phase systems. Adv Protein Chem 24:309–341.
25. Izutsu K, Kojima S. 2000. Freeze-concentration separates proteins and polymer excipients into different amorphous phases. Pharm Res 17:1316–1322.
26. Tolstoguzov VB. 1988. Concentration and purification of proteins by means of two-phase systems: Membraneless osmosis process. Food Hydrocolloids 2:195–207.
27. Izutsu K, Kojima S. 2000. Phase separation of polyelectrolytes and non-ionic polymers in frozen solutions. Phys Chem Chem Phys 2:123–127.
28. Johnson RE, Kirchhoff CF, Gaud HT. 2002. Mannitol-sucrose mixtures—Versatile formulations for protein lyophilization. J Pharm Sci 91:914–922.
29. Dong J, Hubel A, Bischof JC, Aksan A. 2009. Freezing-induced phase separation and spatial microheterogeneity in protein solutions. J Phys Chem B 113:10081–10087.
30. Fonseca F, Passot S, Cunin O, Marin M. 2004. Collapse temperature of freeze-dried Lactobacillus bulgaricus suspensions and protective media. Biotechnol Prog 20:229–238.
31. Zaslavsky BY. 1995. Aqueous two-phase partitioning. 1st edition. New York: Marcel Dekker.
32. Newman A, Engers D, Bates S, Ivanisevic I, Kelly RC, Zografi G. 2008. Characterization of amorphous API:polymer mixtures using X-ray powder diffraction. J Pharm Sci 97:4840–4856.
33. Wang DQ, Hey JM, Nail SL. 2004. Effect of collapse on the stability of freeze-dried recombinant factor VIII and alpha-amylase. J Pharm Sci 93:1253–1263.
34. Anchordoquy TJ, Izutsu KI, Randolph TW, Carpenter JF. 2001. Maintenance of quaternary structure in the frozen state stabilizes lactate dehydrogenase during freeze-drying. Arch Biochem Biophys 390:35–41.
35. Tang XC, Nail SL, Pikal MJ. 2005. Freeze-drying process design by manometric temperature measurement: Design of a smart freeze-dryer. Pharm Res 22:685–700.
36. Kramer T, Kremer DM, Pikal MJ, Petre WJ, Shalaev EY, Gatlin LA. 2008. A procedure to optimize scale-up for the primary drying phase of lyophilization. J Pharm Sci 98:307–318.
37. De Beer TR, Allesø M, Goethals F, Coppens A, Heyden YV, De Diego HL, Rantanen J, Verpoort F, Vervaet C, Remon JP, Baeyens WR. 2007. Implementation of a process analytical technology system in a freeze-drying process using Raman spectroscopy for in-line process monitoring. Anal Chem 79: 7992–8003.
38. Gieseler H, Kessler WJ, Finson M, Davis SJ, Mulhall PA, Bons V, Debo DJ, Pikal MJ. 2007. Evaluation of tunable diode laser absorption spectroscopy for in-process water vapor mass flux measurements during freeze drying. J Pharm Sci 96:1776–1793.

Journal of Chromatography B, 878 (2010) 1466–1470

Contents lists available at ScienceDirect

Journal of Chromatography B

journal homepage: www.elsevier.com/locate/chromb

Analysis of intracellular doxorubicin and its metabolites by ultra-high-performance liquid chromatography

Kumiko Sakai-Kato*, Eiko Saito, Keiko Ishikura, Toru Kawanishi

Division of Drugs, National Institute of Health Sciences, 1-18-1 Kamiyoga, Setagaya-ku, Tokyo 158-8501, Japan

ARTICLE INFO

Article history:
Received 28 February 2010
Accepted 19 March 2010
Available online 27 March 2010

Keywords:
Ultra-high-performance liquid chromatography
Doxorubicin
Doxorubicinol

ABSTRACT

Doxorubicin, a highly effective anticancer drug, produces severe side effect such as cardiotoxicity, which is mainly caused by its metabolite, doxorubicinol. While *in vitro* studies by measuring cellular concentration of doxorubicin have been reported, there have been no reports on measuring cellular concentration of the metabolites. In this report, we developed a sensitive and high-throughput method for measuring cellular concentrations of doxorubicin and its metabolites by ultra-high-performance liquid chromatography. The method achieved more than 96% recovery of doxorubicin and its metabolites from cell homogenates. Using simple separation conditions, doxorubicin and its three main metabolites, and the internal standard, were separated within 3 min. The method has a limit of quantification of 17.4 pg (32.0 fmol) injected doxorubicin. This high sensitivity enables the detection and intracellular quantification of doxorubicin and its metabolite, doxorubicinol, in cell homogenates, and its use will facilitate studies of the relationship between doxorubicin pharmacokinetics and therapeutic outcome.

1. Introduction

The anthracycline doxorubicin, which was originally produced by *Streptomyces peucetius* var. *caesius*, is one of the most widely used anticancer agents, and it has a broad spectrum of activity against a variety of malignancies [1,2]. However, the clinical use of doxorubicin is limited by the side effect of cumulative dose-dependent irreversible chronic cardiomyopathy by doxorubicin and its metabolite, and optimal dose schedules remain a matter of debate [3]. *In vitro* studies have demonstrated a relationship between intracellular doxorubicin levels and cytotoxicity [4,5]. It was proposed that monitoring of intracellular doxorubicin concentrations could help elucidate the relationship between anthracycline pharmacokinetics and therapeutic outcome [6]. Although doxorubicinol, which is one of the major metabolites, has more potent cardiotoxic action than doxorubicin [3], there have been no reports on measuring intracellular level of doxorubicinol, probably due to the detection sensitivity. In this report, we developed a method for measuring intracellular concentrations of doxorubicin and its metabolites.

A number of methods for the simultaneous quantification of doxorubicin and its metabolites in biological samples are based on high-performance liquid chromatography (HPLC) with fluorescence detection [7–11]. Efforts to quantify anthracycline drugs in blood and tissues have encountered methodological difficulties, possibly because of a combination of failure to achieve chromatographic resolution of the various metabolites and the high affinity of these drugs for cellular constituents [12].

Ultra-high-performance liquid chromatography (UHPLC) is a new category of separation techniques that is based upon well-established principles of liquid chromatography. The resolution, sensitivity, and speed of analysis are dramatically increased by the use of 2-μm particles in the stationary phase, high linear velocities for the mobile phase, and instrumentation that operates at higher pressures than those used in HPLC [13–15].

Because doxorubicin intercalates into DNA, to achieve good recovery we used two enzymes during sample preparation that are commonly employed in the purification and degradation of DNA. By using UHPLC, we developed a simple and high-throughput method with high sensitivity for the analysis of intracellular doxorubicin and its metabolites.

2. Materials and methods

2.1. Drugs and chemicals

Doxorubicin hydrochloride and daunorubicin hydrochloride were purchased from Wako Pure Chemical Industries, Ltd. (Osaka,

Abbreviations: UHPLC, ultra-high-performance liquid chromatography; PMSF, phenylmethylsulfonyl fluoride; Triton X-100, polyoxyethylene(10) octylphenyl ether; DMEM, Dulbecco's modified Eagle's medium; FBS, fetal bovine serum.

* Corresponding author. Tel.: +81 3 3700 9662; fax: +81 3 3700 9662.
E-mail address: kumikato@nihs.go.jp (K. Sakai-Kato).

1570-0232/$ – see front matter © 2010 Elsevier B.V. All rights reserved.
doi:10.1016/j.jchromb.2010.03.040

Japan). Doxorubicinol hydrochloride and doxorubicinone were purchased from Toronto Research Chemicals Inc. (North York, Canada). Doxorubicinolone was synthesized from doxorubicinol by acidic hydrolysis (0.5 N HCl) at 50 °C for 24 h. Aglycone was extracted with chloroform by a liquid–liquid extraction method [16].

DNase I, phenylmethylsulfonyl fluoride (PMSF), proteinase K, and zinc sulfate heptahydrate were obtained from Sigma–Aldrich Corporation (St. Louis, MO, USA). Polyoxyethylene(10) octylphenyl ether (Triton X-100), magnesium chloride, sodium dihydrogen phosphate dehydrate, and phosphoric acid were obtained from Wako Pure Chemical Industries, Ltd. HPLC-grade isopropanol, HPLC-grade acetonitrile, and HPLC-grade methanol were obtained from Kanto Chemical Co., Inc. (Tokyo, Japan).

2.2. Cell culture

HeLa cells (Health Science Research Resources Bank, Osaka, Japan) and HT29 cells (American Type culture Collection, VA, USA) were cultured in Dulbecco's modified Eagle's medium (DMEM; Invitrogen Corp., CA, USA) supplemented with 10% fetal bovine serum (FBS; Nichirei Biosciences Inc., Tokyo, Japan) and 100 U/mL penicillin–streptomycin mixture (Invitrogen). Cells were grown in a humidified incubator at 37 °C and 5% CO_2.

2.3. Preparation of samples for HPLC

Cells were washed with PBS, resuspended in 300 μL PBS and lysed on ice with an ultrasonic homogenizer (Astrason, Misonix Inc., IN, USA). The lysed samples were treated with enzymes according to the method of Anderson et al. [4]. Five microliters Triton X-100 (5%) and 5 μL proteinase K (10 mg/mL) were added to an aliquot of 200 μL cell homogenates. After brief mixing, the samples were incubated for 1 h at 65 °C in a water bath. An aliquot of 2.5 μL PMSF (10 mM in isopropanol) was added and the samples were incubated for 10 min at room temperature. Then 5 μL $MgCl_2$ (0.4 M) and 10 μL DNase I (1 mg/ml) were added and the samples were incubated in a water bath at 37 °C for 30 min.

Each 225 μL sample was then mixed with 225 μL methanol and 22.5 μL $ZnSO_4$ (400 mg/mL) and centrifuged at 15,000 × *g* for 5 min in a microcentrifuge (Model 3740, Kubota Corp., Tokyo, Japan); the supernatants were then collected. A 30-μL aliquot of each supernatant was mixed with 5 μL of the internal standard (daunorubicin, 10 μg/mL in methanol), 50 μL ice-cold methanol and 15 μL Milli-Q water, and filtered through a 0.20-μm filter (Millex-LG, Millipore Corp., Tokyo, Japan). The filtrates were transferred to autosampler vials before UHPLC analysis.

The amounts of protein in cell homogenates were determined using BIO-RAD protein assay reagent (BIO-RAD, CA, USA).

2.4. HPLC apparatus

High-throughput quantification of doxorubicin and its metabolites was performed using a Hitachi LaChrom ULTRA system, equipped with an L-2160U pump, an L-2200U automated sample injector, an L-2300 thermostatted column compartment, and an L-2485U fluorescence detector (Hitachi, Tokyo, Japan).

2.5. Chromatographic conditions

Samples were analyzed on a Capcell Pak C18 IF column (2.0 × 50 mm; particle size, 2 μm; Shiseido Corp., Tokyo, Japan). The mobile phase consisted of a 50-mM sodium phosphate buffer (pH 2.0): acetonitrile mixture (65:27 v/v). The mobile phase was delivered at a rate of 300 μL/min and the column temperature was maintained at 25 °C. The fluorescence detector was operated at an excitation wavelength of 470 nm and an emission wavelength of 590 nm. A volume of 5 μL of sample was injected each time.

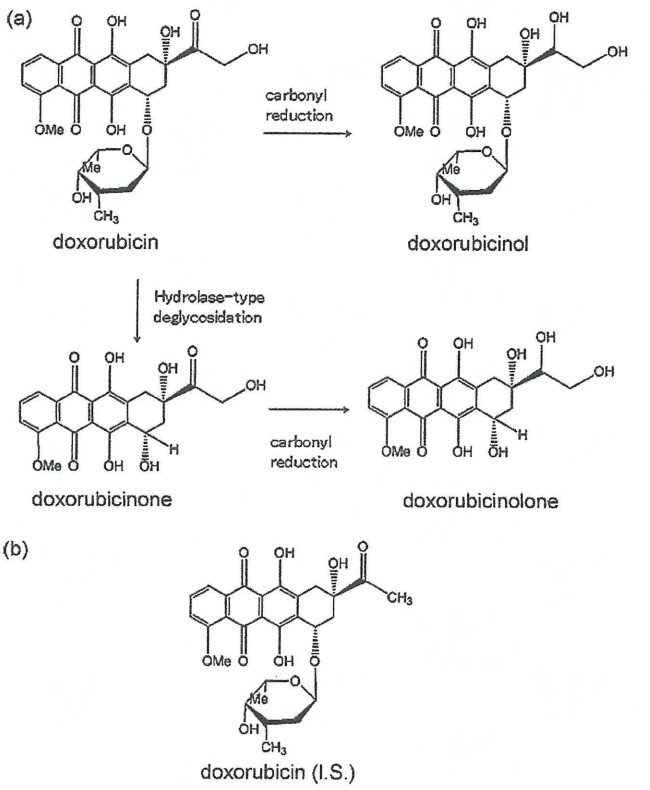

Fig. 1. Schematic showing the chemical structure of doxorubicin and its metabolites (a) and the chemical structure of daunorbicin, the internal standard (b).

2.6. Confocal analysis of live cells

The intracellular distribution of doxorubicin was examined by live-cell confocal microscopy (Carl Zeiss LSM 510, Germany). Dedicated software supplied by the microscope manufacturers was used to collect data, and images were exported as TIFF files. HeLa cells (1.5×10^5) were plated into 35-mm glass-bottomed dishes coated with poly-L-lysine (Matsunami, Osaka, Japan) and cultured in DMEM containing 10% FBS and 100 U/mL penicillin–streptomycin mix. After 2 days of incubation (37 °C, 5% CO_2), the culture medium was replaced and the cells were exposed to 1 μg/mL doxorubicin. After 1 h, cells were washed and kept in Hanks's Balanced Salt Solution (Invitrogen) for subsequent imaging by confocal microscopy.

3. Results and discussion

3.1. Chromatograms

Fig. 1a shows the chemical structure of doxorubicin and the doxorubicin metabolites that were studied in this report, and the structure of the internal standard (daunorubicin) (Fig. 1b). Because these chemicals show native fluorescence, they can be sensitively analyzed by the detection of this fluorescence. Fig. 2 shows the chromatograms resulting from the analysis of a standard solution of doxorubicin, doxorubicinol, doxorubicinolone, doxorubicinone, and the internal standard. All compounds were separated within 3 min with good resolution owing to the use of UHPLC. The pressure was 26.6 MPa at a flow rate of 300 μL/min, but the pressure was not high enough to adversely affect the stability of the column. High repeatability of analyte retention times was achieved; the relative

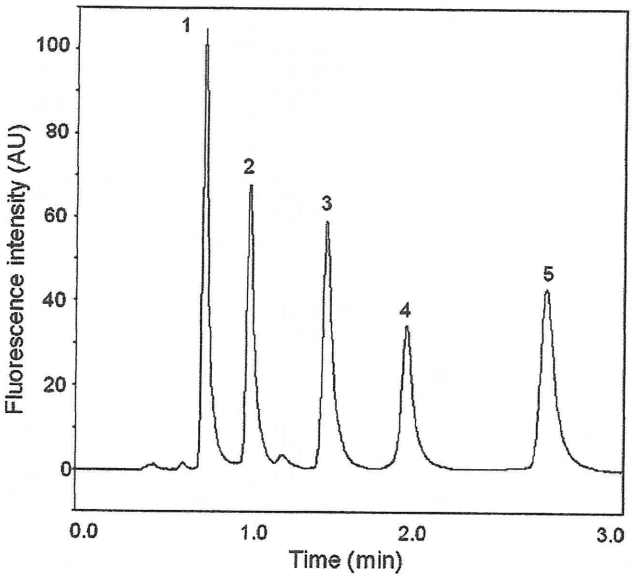

Fig. 2. Chromatogram of doxorubicin and its metabolites. The chromatographic conditions are described in Section 2. 1, doxorubicinol; 2, doxorubicin; 3, doxorubicinolone; 4, daunorubicin (internal standard); 5, doxorubicinone.

standard deviation (R.S.D.) of each peak was less than 0.13% ($n = 5$), for each analyte, at a concentration of 50 ng/mL. The conditions of separation of doxorubicin and its three metabolites were very simple in that the elution was isocratic, and the mobile phase consisted of only two different solvents, whereas some reported methods require three different solvents [7,8]. Fig. 3a is a chromatogram of a homogenate from untreated HeLa cells, and Fig. 3b is a chromatogram of an equivalent homogenate spiked with doxorubicin and its metabolites at a concentration of 500 ng/mL. No interfering peaks were observed, and doxorubicin, the three metabolites, and the internal standard separated well. These results show that the separation conditions were optimized with selectivity to each compound.

3.2. Detection limits and quantitation limits

Detection limits and quantitation limits of doxorubicin and its metabolites were determined based on the signal-to-noise approach, (S:N ratio, 3:1 for detection limits and 10:1 for quantitation limit) (Table 1). The quantitation limits of doxorubicin, doxorubicinol, doxorubicinolone, and doxorubicinone ranged between 11.7 and 24.5 pg/injection. The quantitation limit of 17.4 pg/injected doxorubicin (32.0 fmol/injected doxorubicin) was about 2 times lower than the limit ever reported using conventional HPLC [8], and more than 10 times lower than other reported values [7,9–11]. We suggest that the high resolution and sensitivity of UHPLC are responsible for this improvement.

Table 1
Detection limits and quantitation limits of doxorubicin and its metabolites.

Compound	Detection limit (pg/injection)	Quantitation limit (pg/injection)
Doxorubicin	5.2	17.4
Doxorubicinol	3.5	11.7
Doxorubicinolone	6.0	19.8
Doxorubicinon	7.4	24.5

The detection and quantitation limits of doxorubicin and its metabolites were determined based on signal-to-noise ratios (3:1 for detection limits, and 10:1 for quantitation limits).

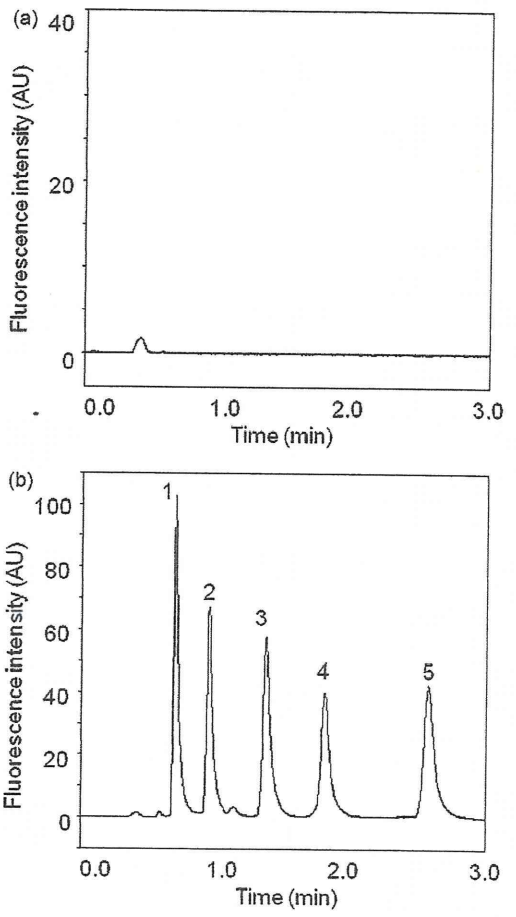

Fig. 3. Chromatograms of (a) HeLa cell homogenate and (b) HeLa cell homogenate spiked with doxorubicin and its metabolites. The chromatographic conditions were the same as in Fig. 2 and are described in Section 2. 1, doxorubicinol; 2, doxorubicin; 3, doxorubicinolone; 4, daunorubicin (internal standard); 5, doxorubicinone.

3.3. Drug recovery

Doxorubicin and its metabolites have a high affinity for cellular constituents [12]. Confocal fluorescence imaging of a HeLa cell that was exposed to doxorubicin for 1 h showed that doxorubicin had preferential affinity for the nucleus (Fig. 4). Drug recovery was assessed by adding doxorubicin, doxorubicinol, doxorubicinolone,

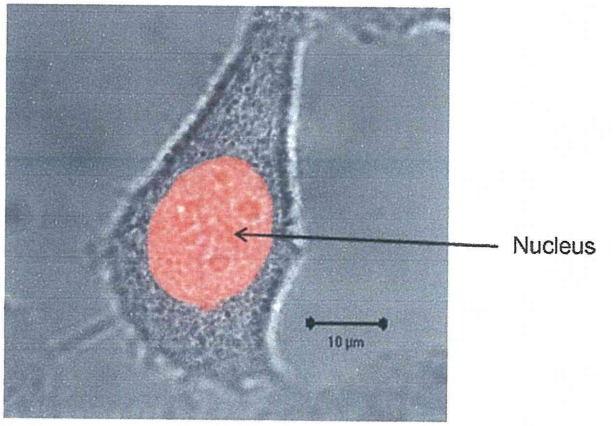

Fig. 4. Intracellular distribution of doxorubicin. HeLa cells were exposed to 1 μg/mL doxorubicin for 1 h, washed, and observed by confocal microscopy. Scale bar: 10 μm.

Table 2
The recovery of doxorubicin and its metabolites from HeLa cell homogenates.

Compound	Recovery rate	
	(%)	R.S.D. (%)
Doxorubicin	102	3.3
Doxorubicinol	105	2.9
Doxorubicinolone	96	1.4
Doxorubicinone	98	2.1

Each compound (1 μg/mL) was added to HeLa cell homogenates, which were then treated as described in Section 2. Mean values for percentage recovery are given ($n=3$).

and doxorubicinone to homogenates of two representative human cancer cell-lines, HeLa cells (derived from human epithelial carcinoma) and HT29 cells (derived from human colon adenocarcinoma grade II) before sample preparation. When the cell homogenate was treated with only methanol and $ZnSO_4$, by a method previously used to study doxorubicin and its metabolites in plasma [9], the percentage recoveries of doxorubicin, doxorubicinol, doxorubicinolone, and doxorubicinone were 84.1 ± 8.2%, 63.2 ± 3.0%, 78.4 ± 3.7%, and 88.7 ± 2.7%, respectively, ($n=3$). Doxorubicinol is harder to recover because it has higher affinity to the cellular constituents, and this affinity to the cellular constituents causes its cytotoxicity [3]. To obtain a higher drug recovery, the cells were lysed by an ultrasonic homogenizer, and the cellular proteins were further digested and solubilized with a combination of Triton X-100 and the endopeptidase proteinase K. Nuclear DNA was hydrolyzed by treatment with DNase I in the presence of divalent cations. Using these enzymatic treatments in accordance with the method of Anderson et al. [4], the recovery dramatically improved (Table 2). Furthermore, for each compound, a satisfactory within-day repeatability was achieved with R. S. D. of ≤ 3.3%, $n=3$.

3.4. Linearity of the calibration plots

We created calibration plots for doxorubicin, doxorubicinol, doxorubicinolone, and doxorubicinone (Fig. 5). The *y*-axis is the ratio of the peak area of each analyte tested to the peak area of the internal standard (daunorubicin), and the *x*-axis is the concentra-

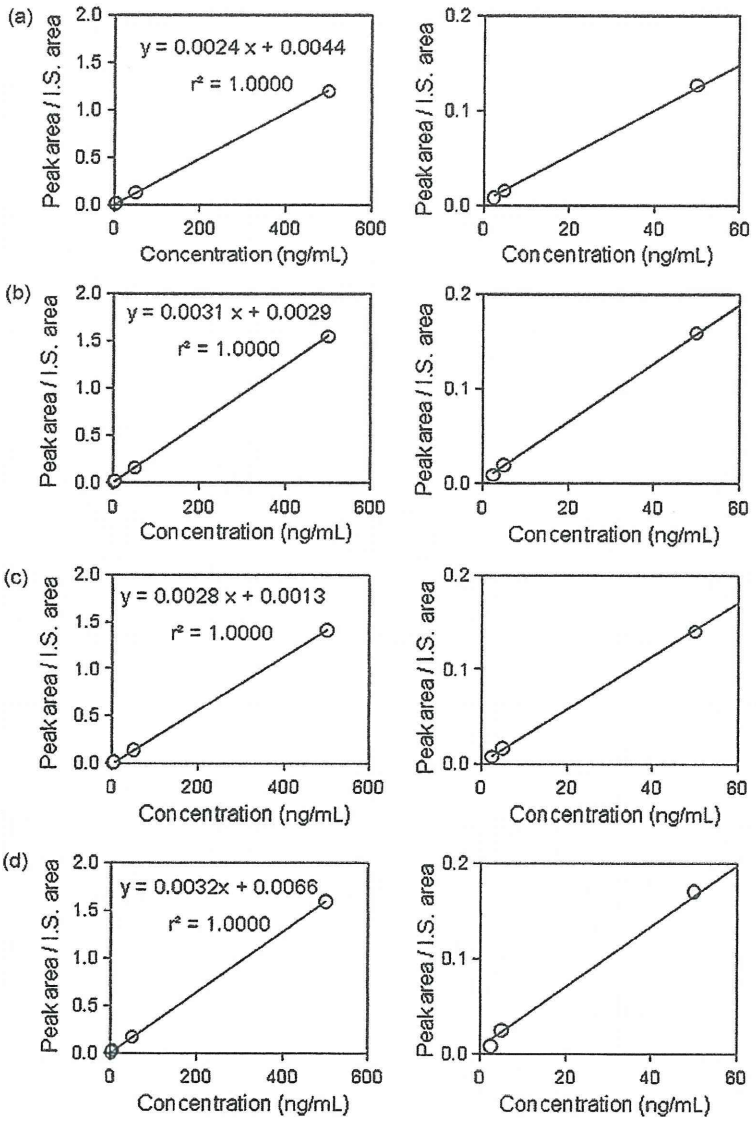

Fig. 5. Linearity of the calibration curves of doxorubicin and its metabolites. Calibration plots for (a) doxorubicin, (b) doxorubicinol, (c) doxorubicinolone, and (d) doxorubicinone. The left and right panels show results for the same HPLC run, but the plots in the right panel focus on the lower concentration ranges. I.S. denotes internal standard.

Table 3
Quantitation of doxorubicin and doxorubicinol in homogenates prepared from doxorubicin-treated cells.

Sample	Doxorubicin (μg/mg cell protein)	Doxorubicinol (μg/mg cell protein)
HeLa cells	3.4 ± 0.55	0.057 ± 0.0060
HT29 cells	3.5 ± 0.38	0.048 ± 0.0029

Cells were treated for 2 h with 10 μg/mL doxorubicin, and cell homogenates were prepared and analyzed, as described in Section 2. Values are given as mean ± S.D. (n (dish number) = 3).

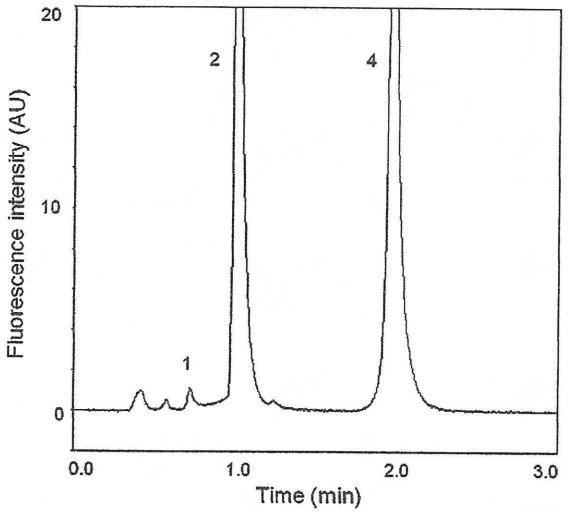

Fig. 6. Chromatogram of cell homogenate obtained 2 h after administration of doxorubicin. HeLa cells were exposed to 10 μg/mL doxorubicin for 2 h. Cell homogenates were then prepared as described in Section 2. 1, doxorubicinol; 2, doxorubicin; 3, daunorubicin (internal standard).

tion of the corresponding analyte. The plots were linear over a wide range of concentrations (r^2 = 1.0; Fig. 5).

3.5. *Quantitative determination of the levels of doxorubicin and its metabolite in cells*

The validated method described above was used for the simultaneous determination of doxorubicin and its metabolites in human cancer cell-lines. HeLa cells and HT29 cells were exposed to 10 μg/mL doxorubicin for 2 h, and then washed with PBS. Chromatograms of the cell homogenates were obtained by UHPLC (Fig. 6). As shown, doxorubicin and one of its metabolites, doxorubicinol, were detected in cell homogenates (Fig. 6). The results of quantitative determination of doxorubicin and doxorubicinol are shown in Table 3. Values are expressed as amounts per 1 mg cellular protein in each dish, due to the diversity of cell numbers for different dishes, and values are given as mean ± S.D. for three dishes of the same cell type. The S.D. values for different dishes of the same cell type were acceptable. Doxorubicinol is produced by cytosolic carbonyl reductase through the NADPH-dependent aldo-keto reduction of a carbonyl moiety in doxorubicin [17]; our results first demonstrated that both human cancer cell-lines, HeLa cells and HT29 cells, produced doxorubicinol from doxorubicin. In contrast, our results showed that deglycosidation at the daunosamine sugar in doxorubicin, which produces doxorubicinone and doxorubicinolone (Fig. 1a) [17], was negligible in these cancer cell-lines (Fig. 6).

New formulation technologies that aim to enhance the effectiveness and safety of anticancer drugs are currently being developed. For instance, long-circulating and sterically stabilized liposomes containing doxorubicin can markedly increase tumor-specific deposition of drugs and have been approved as clinical products [18]. Other carrier systems such as polymer micelles [19,20] are also being developed for use with doxorubicin. In these technologies, effective release of doxorubicin from the carrier into the target cells is important for effectiveness and safety. Direct quantification of the metabolites may facilitate the assessment and comparison of doxorubicin release from carriers, since it is presumed that metabolism of doxorubicin takes place only after its release from the carriers. Analytical methodology that enables the rapid quantification of doxorubicin and its metabolites, particularly in targeted tumor cells, will facilitate the optimization of carrier-based strategies for doxorubicin delivery and will help provide insight into the toxicity and bioavailability of doxorubicin incorporated into carriers such as liposomes or polymer micelles.

4. Conclusions

Our results show that this methodology provides a significant reduction in analysis time and a considerable increase in assay sensitivity. We demonstrated that the method is sensitive enough to quantify the levels of doxorubicin and its metabolite within cells, and we predict that it will greatly facilitate studies of doxorubicin pharmacokinetics and clarify the effect of doxorubicin metabolism on therapeutic outcome at the cellular level. Furthermore, this method can be applied to the evaluation of emerging formulation technologies that are based on encapsulated doxorubicin.

Acknowledgements

The authors are grateful for financial support from the Research on Publicly Essential Drugs and Medical Devices Project (The Japan Health Sciences Foundation), a Health Labor Sciences Research Grant from the Ministry of Health, Labour and Welfare (MHLW), and KAKENHI (21790046) from the Ministry of Education, Culture, Sports, Science, and Technology (MEXT), Japan.

References

[1] G.N. Hortobagyi, Drugs 54 (1997) 1.
[2] A. Di Marco, M. Gaetani, B. Scarpinato, Cancer Chemother. Rep. 53 (1969) 33.
[3] R.D. Olson, P.S. Mushlin, D.E. Brenner, S. Fleischer, B.J. Cusack, B.K. Chang, R.J. Boucek Jr., Proc. Natl. Acad. Sci. U.S.A. 85 (1988) 3585.
[4] A. Anderson, D.J. Warren, L. Slordal, Cancer Chemother. Pharmacol. 34 (1994) 197.
[5] S. Licata, A. Saponiero, A. Mordente, G. Minotti, Chem. Res. Toxicol. 13 (2000) 414.
[6] B. Sundman-Engberg, U. Tidefelt, J. Liliemark, C. Paul, Cancer Chemother. Pharmacol. 25 (1990) 252.
[7] Q. Zhou, B. Chowbay, J. Pharm. Biomed. Anal. 30 (2002) 1063.
[8] J.V. Aspere, O.V. Tellingen, J.H. Beijnen, J. Chromatogr. B: Biomed. Sci. Appl. 712 (1998) 129.
[9] A. Andersen, D.J. Warren, L. Slordal, Ther. Drug Monit. 15 (1993) 455.
[10] S. Shinozawa, Y. Mimaki, Y. Araki, T. Oda, J. Chromatogr. 196 (1980) 463.
[11] L.M. Rose, K.F. Tillery, S.M. el Dareer, D.L. Hill, J. Chromatogr. 425 (1988) 419.
[12] A. Andersen, H. Holte, L. Slordal, Cancer Chemother. Pharmacol. 44 (1999) 422.
[13] M.E. Swartz, J. Liq. Chromatogr. Relat. Technol. 28 (2005) 1253.
[14] L. Novakova, H. Vlckova, Anal. Chim. Acta 656 (2009) 8.
[15] N. Sun, G. Lu, M. Lin, G. Fan, Y. Wu, Talanta 78 (2009) 506.
[16] K.E. Maudens, C.P. Stove, W.E. Lambert, J. Sep. Sci. 31 (2008) 1042.
[17] S. Takanashi, N.R. Bachur, Drug Metab. Dispos. 4 (1976) 79.
[18] M.E.R. O'Brien, N. Wigler, M. Inbar, R. Rosso, E. Grischke, A. Santoro, R. Catane, D.G. Kieback, P. Tomczak, S.P. Ackland, F. Orlandi, L. Mellars, C. Tendler, Ann. Oncol. 15 (2004) 440.
[19] M. Yokoyama, T. Okano, Y. Sakurai, S. Fukushima, K. Okamoto, K. Kataoka, J. Drug Target. 7 (1999) 171.
[20] T. Nakanishi, S. Fukushima, K. Okamoto, M. Suzuki, Y. Matsumura, M. Yokoyama, T. Okano, Y. Sakurai, K. Kataoka, J. Control. Release 74 (2001) 295.

RESEARCH ARTICLE

Stabilization of Liposomes in Frozen Solutions Through Control of Osmotic Flow and Internal Solution Freezing by Trehalose

KEN-ICHI IZUTSU, CHIKAKO YOMOTA, TORU KAWANISHI

National Institute of Health Sciences, Setagaya-ku, Tokyo 158-8501, Japan

Received 22 September 2010; revised 7 December 2010; accepted 25 January 2011

Published online in Wiley Online Library (wileyonlinelibrary.com). DOI 10.1002/jps.22518

ABSTRACT: The purpose of this study was to elucidate the effect of trehalose distribution across the membrane on the freeze-related physical changes of liposome suspensions and their functional stability upon freeze–thawing. Cooling thermal analysis of 1,2-dipalmitoyl-*sn*-glycero-3-phosphocholine liposome suspensions showed exotherm peaks of bulk (−15°C to −25°C) and intraliposomal (approx. −45°C) solution freezing initiated by heterogeneous and homogeneous ice nucleation, respectively. The extent of the intraliposomal solution freezing exotherm depended on liposome size, lipid composition, cosolutes, and thermal history, suggesting that osmotic dehydration occurred due to the increasing difference in solute concentrations across the membrane. A freeze–thawing study of carboxyfluorescein-encapsulated liposomes suggested that controlling the osmotic properties to avoid the freeze-induced intraliposomal solution loss either by rapid cooling of suspensions containing trehalose in both sides of the membrane (retention of the intraliposomal supercooled solution) or by cooling of suspensions containing trehalose in the extraliposomal media prior to freezing (e.g., osmotic shrinkage) led to higher retention of the water-soluble marker. Evaluation and control of the osmotically mediated freezing behavior by optimizing the formulation and process factors should be relevant to the cryopreservation and freeze-drying of liposomes. © 2011 Wiley-Liss, Inc. and the American Pharmacists Association J Pharm Sci

Keywords: liposomes; formulation; stabilization; thermal analysis; osmosis; calorimetry (DSC); excipients; freeze-drying

INTRODUCTION

The increase in the variety and clinical relevance of liposomal formulations has enhanced the importance of the freezing and freeze-drying processes for the distribution and long-term storage of the drug delivery systems that are not chemically and/or physically stable enough as aqueous suspensions.[1–4] These processes, however, expose the lipid systems to various stresses including ice growth, pH change, concentration of the surrounding solutes, and dehydration that often damage their structural integrity and pharmaceutical functions [e.g., release of active pharmaceutical ingredients (APIs)] of liposomes. Retaining water-soluble APIs is a particular challenge for development of liposome formulations.[1] Formulation and process design that are based on an understanding of the freeze-related stresses and required stabilization mechanisms should improve the stability of various liposome pharmaceuticals.[1–3]

Disaccharides (e.g., trehalose and sucrose) and some amino acids have been applied to protect the lipid systems from chemical and physical changes during freeze–thawing (cryoprotectants) and freeze-drying (lyoprotectants).[1,3] The stabilization of liposomes by disaccharides is explained mainly by three mechanisms. Some saccharides substitute the water molecules necessary to retain the supramolecular phospholipid assembly through molecular interactions with hydrophilic phospholipid head groups (water substitution).[5–7] The saccharides also form highly viscous amorphous freeze-concentrated phases and dried solids that prevent direct contact between liposome vesicles (bulking).[1,8,9] The reduced mobility of the surrounding molecules helps improve the chemical and physical stability of liposomes (vitrification). Use of the stabilizers is mostly dependent on empirical trial and error through analysis of the morphological (e.g., size) and functional (e.g., API or marker

Correspondence to: Ken-ichi Izutsu (Telephone: +81-3-3700-1141; Fax: 81-3-3707-6950; E-mail: izutsu@nihs.go.jp)

Journal of Pharmaceutical Sciences

retention) traits of the resulting suspensions or dried solids.

Longstanding cryopreservation studies of living cells and microorganisms provide precepts valuable for the protection of liposomes against the freeze-induced stresses.[10–14] The cooling of cell and liposome suspensions induces the freezing of bulk solutions initiated by heterogeneous ice nucleation at the surface of containers or impurities (−5°C to −25°C) and the freezing of spatially restricted internal solutions initiated by homogeneous (spontaneous) ice nucleation (−25°C to −45°C).[15–21] The bulk solution freezing and the accompanying significant concentration of solutes surrounding the living cells and liposomes induce osmotic stress that removes the internal solution before they freeze, leading to morphological changes observable by microscopic methods (e.g., optical microscope and cryo-transmission electron microscopy).[21,22] Because the intracellular ice formation (IIF) is widely recognized to cause lethal damage through disordering of the complex membrane and intracellular structure (e.g., organelle), cryopreservation of the living cells and microorganisms is usually performed in two ways that prevent IIF, namely by slow cooling of suspensions containing extracellular solutes (cell dehydration) and by rapid cooling of the suspensions containing high-concentration membrane-permeating solutes [e.g., dimethyl sulfoxide (DMSO), cytoplasm vitrification].[12] On the contrary, only limited studies have been performed on the stabilization of liposomes taking various freezing-related physical changes into account.[17,23–25]

The purpose of this study was to elucidate the effect of intra- and extraliposomal trehalose on the freeze-related physical changes and functional stability of liposomes during freeze–thawing. The effect of saccharide distribution across the membrane on the stability of liposomes is of particular interest for formulation purposes because the liposome preparation methods significantly affect allocation of the nonpermeating solutes. Different solute concentrations across the membrane induce osmotic flow that shrinks or swells the liposomes in the aqueous suspensions.[4,22,26] Literature claims the requirement of disaccharides on both sides of the membrane to protect liposomes from freezing- and lyophilization-related stresses (e.g., addition before extrusion).[8] Recent reports suggested that the rational setting of different intra- and extraliposomal trehalose concentrations confers better stabilization.[1,27] Effect of trehalose on the freeze-related physical phenomena (e.g., freeze-induced dehydration and intraliposomal solution freezing) and functional stability of liposomes were studied mainly through thermal analysis and through the retention of encapsulated carboxyfluorescein (CF).[27,17]

MATERIALS AND METHODS

Materials

Chemicals obtained from the following sources were used without further purification: 1-palmitoyl-2-oleoyl-*sn*-glycero-3-phosphocholine (POPC), 1,2-dimyristoyl-*sn*-glycero-3-phosphocholine (DMPC), 1,2-dipalmitoyl-*sn*-glycero-3-phosphocholine (DPPC), and 1,2-distearoyl-*sn*-glycero-3-phosphocholine (DSPC) (NOF Co., Tokyo, Japan); trehalose dihydrate, glucose, sucrose, and 5(6)-CF (Sigma–Aldrich Co., St. Louis, Missouri); DMSO, xylitol, and glycerol (Wako Pure Chemical Co., Osaka, Japan); and dextran 4000–6000 (Serva Electrophoresis GmbH, Heidelberg, Germany).

Preparation of Liposome Suspensions

Phospholipid films were obtained by drying their solution in a chloroform and methanol mixture (2:1) under vacuum at temperatures above the main transition temperature (T_m). Liposome suspensions were prepared by using a hand-held extruder (Avanti Polar Lipids, Alabaster, Alabama). The films hydrated by 10 mM Tris–HCl buffer (6%, w/w; pH 7.4) were extruded 12 times through a polycarbonate membrane filter (0.1–0.8 μm pore, 0.2 μm unless otherwise mentioned; Whatman, Maidstone, UK) while maintaining the apparatus at room temperature (POPC) or at temperatures 10 to 15°C higher than the T_m of the respective lipids. The DPPC liposomes extruded through the smaller pore membranes (0.1 and 0.2 μm) were reported to have a unilamellar structure, whereas those extruded through the larger pore membranes (0.4 and 0.8 μm) contained increasing ratios of multilamellar vesicles.[29,30] The term "0.2 μm liposome" will be used in the text given below to denote samples prepared by extrusion through the respective pore size membranes.

Some liposome suspensions containing the excipients predominantly in the extraliposomal media were prepared by adding the excipients approximately 30 min prior to the thermal analysis and freeze–thawing experiments. Those containing excipients in both the inside and outside of the membranes were prepared by the extrusion of lipids hydrated with the excipient-containing solutions. Some suspensions were eluted through Sephadex G-25 desalting columns (PD-10; GE Healthcare Bio-Sciences AB, Uppsala, Sweden) equilibrated with the Tris–HCl buffer to obtain samples containing the excipient mainly in the intraliposomal solutions. The concentrations of DPPC in the column-eluted suspensions were obtained by phosphorous assay.[31] Measurement of the DPPC concentrations in the liposome suspensions indicated that approximately 90% of the liposomes passed through the Sephadex columns.

DOI 10.1002/jps

Thermal Analysis

Thermal analysis of the frozen liposome suspensions was performed by using a differential scanning calorimeter (DSC Q10; TA Instruments, New Castle, Delaware) equipped with a refrigerating system and data processing software (Universal Analysis 2000, TA Instruments). Aliquots [10 μL, 4% (w/w) lipid] of suspensions in hermetic aluminum cells were cooled from 25°C to −70°C at varied speeds (1–10°C/min) and then heated to 25°C at a scanning rate of 5°C/min. The intensity of the intraliposomal solution freezing exotherm was shown as their ratio to the lipid content (J/g lipid). Some DPPC liposome suspensions were heat-treated at 45°C for 3 min before the cooling scan. The cooling scan of some suspensions were paused at certain temperatures (−10°C to −35°C) and maintained those temperatures for 30 or 60 min before further cooling to study the effect of low temperature storage on the physical changes. The column-eluted liposome suspensions were subjected to thermal analysis without the concentration adjustment. The homogeneous ice formation exotherms of these suspensions were calculated using the phosphate concentration data.

Measurement of Liposome Size by Dynamic Light Scattering

The size distribution of liposomes suspended in the Tris–HCl buffer (0.08% DPPC, 25°C) was determined using a dynamic light scattering (DLS) spectrophotometer (Photal DLS-7100SL; Otsuka Electronics Co., Osaka, Japan) with a He–Ne laser (632.8 nm) and a scattering angle (90°; 50 scans).

CF Retention Study

Dried DPPC films were hydrated with solutions containing 25 mM 5(6)-CF, 10 mM Tris–HCl buffer, and 0% or 12% trehalose, adjusted to pH 7.4 by NaOH. The CF-loaded vortexed multilamellar liposome suspensions (6% lipid, w/w) were prepared by extrusion through a 0.2-μm pore filter, and then eluted through the Sephadex G-25 column equilibrated with the buffer or trehalose-containing buffer. Freeze–thawing of the suspension was performed using the DSC system while the thermal profiles were simultaneously monitored. Aliquots of the liposome suspensions (10 μL, 4% DPPC, w/w) in unsealed aluminum pans were cooled to −35°C or −70°C at varied cooling speeds (1–10°C/min), and then heated to 25°C at 10°C/min on the DSC furnace. The freeze–thawed liposome suspensions were diluted by adding the Tris–HCl buffer or trehalose-containing buffer solutions (10 mL) in the glass tubes. The mildly agitated liposome suspensions underwent fluorescence measurement using a spectrometer (FP-6500; JASCO Corp., Tokyo, Japan). After the initial fluorescence measurements of the suspensions (2 mL) at 460 nm (excitation) and 550 nm (emission), those of the membrane-perturbed liposome suspensions were obtained by the addition of aliquots (20 μL) of Triton X-100. The CF leakage ratio was calculated using the following equation:

$$\%\,\text{Leakage} = \frac{\text{Initial fluorescence of treated sample} - \text{initial fluorescence of control}}{(\text{Final fluorescence of treated sample} - \text{initial fluorescence of control})} \times 100$$

RESULTS AND DISCUSSION

Freeze-Induced Changes in Liposome Suspensions

Figure 1 shows a thermogram of a frozen DPPC liposome suspension (4% in 10 mM Tris–HCl buffer, 0.2 μm) cooled at 5°C/min. The suspension showed a large exothermic peak of the freezing of the bulk solution (heterogeneous ice nucleation) at approximately −20°C and a smaller second exothermic peak of the freezing of the intraliposomal solution (homogeneous ice nucleation) at approximately −45°C.[15,17,32] The lower temperature exotherm disappeared by prior addition of a membrane-perturbing surfactant (1% Triton X-100), which supported the aforementioned definition of the peak rather than other interpretations (e.g., freezing of phosphatidylcholine headgroups) of the exotherm (data not shown).[33] The temperature

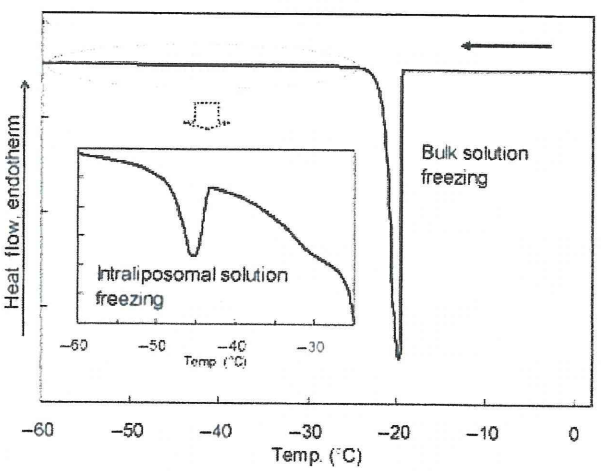

Figure 1. Cooling thermogram of a frozen DPPC liposome suspension. An aliquot (10 μL) of liposome suspension (4% lipid, w/w) in Tris–HCl buffer (10 mM, pH 7.4) was cooled from room temperature to −70°C at 5°C/min.

of the bulk solution freezing peak varied greatly between the scans. Some suspensions also showed a broad exotherm at approximately −30°C. The exotherm suggested the freezing of solutions released from the liposomes (dehydration) and/or freezing of the internal solutions initiated by external ice crystals that penetrated through the membrane.[12,16,34] The varied shape and overlapping of the peak with the large bulk solution freezing exotherm made further characterization difficult in this study. The frozen liposome suspensions showed only a gradual shift of the thermogram before the large ice melting endotherm during their heating scans (data not shown). DLS measurement of the DPPC liposome suspensions indicated a mean diameter of 203.9 ± 10.6 nm before the thermal analysis (three different preparations). Standard deviation of the liposome size obtained in each measurement was within 5% of the average value.

The effects of cooling speeds on the internal solution freezing exotherm of liposomes differing in size and lipid composition are shown in Figure 2. Slower cooling of the DPPC liposome suspension (0.2 μm) reduced the exotherm, indicating loss of the supercooled intraliposomal solution during the scan (Fig. 2a; 1 −2°C/min). The extraliposomal ice growth and concomitant concentration of solutes should generate osmotic forces that induce water evacuation from liposomes. Reported freeze-induced morphological rearrangement into multilamellar liposomes may also reduce the intraliposomal solution content.[4] The width of the bulk solution freezing peak got narrower in the slower cooling, suggesting a certain time required for the ice growth (data not shown). On the contrary, the limited effect of the cooling speed on the peak width of the intraliposomal solution freezing exotherm suggested independent ice formation in the individual liposomes. A certain amount of the intraliposomal solution interacting (hydrating) with the membrane lipid and/or solute molecules should remain unfrozen even below the intraliposomal solution freezing temperature.[11,11]

Reduction of the intraliposomal solution freezing exotherm was more apparent in the DPPC liposome suspensions temporarily (30 min) kept at temperatures between the bulk and the intraliposomal solution freezing during the cooling scan (Fig. 3). The finding that the intraliposomal solution freezing exotherm of a suspension held at −25°C was smaller than those of suspensions held at −30°C or −35°C suggested faster loss of the supercooled solutions in the temperature range just below the bulk solution freezing. Longer exposure to the temperature range should be one of the reasons for the reduction in the exotherms with the slower cooling. On the contrary, holding the suspension at a temperature above the bulk solution freezing temperature showed no apparent effect on the intraliposomal solution freezing

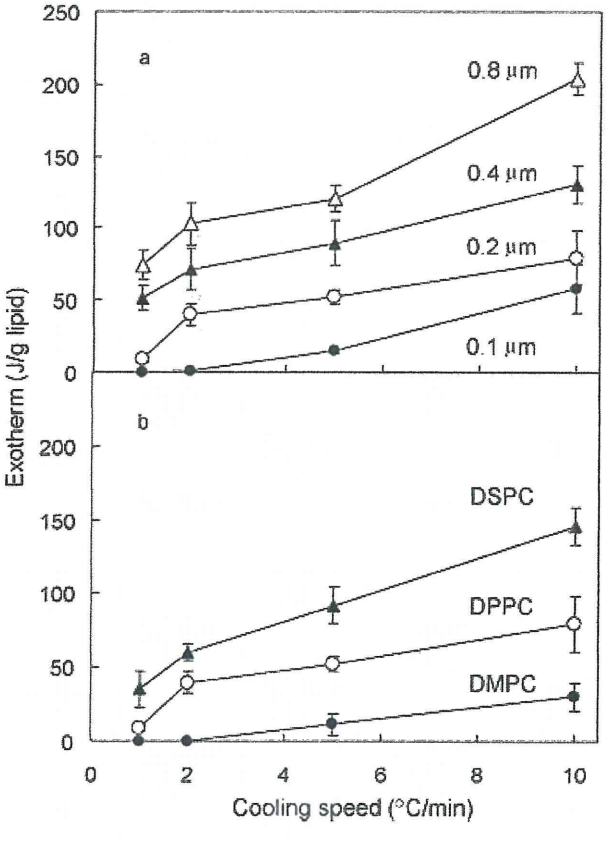

Figure 2. Effects of cooling speed on internal solution freezing exotherm of liposome suspensions with differing (a) extrusion membrane pore sizes (DPPC; 0.1 μm: •, 0.2 μm: ○, 0.4 μm: ▲, and 0.8μm: △) and (b) lipid compositions (0.2 μm; DMPC: •, DPPC: ○, and DSPC: ▲). Aliquots of liposome suspensions (10 μL, 4% lipid in 10 mM Tris–HCl buffer) were cooled at 1–10°C/min (average ± SD, $n = 3$).

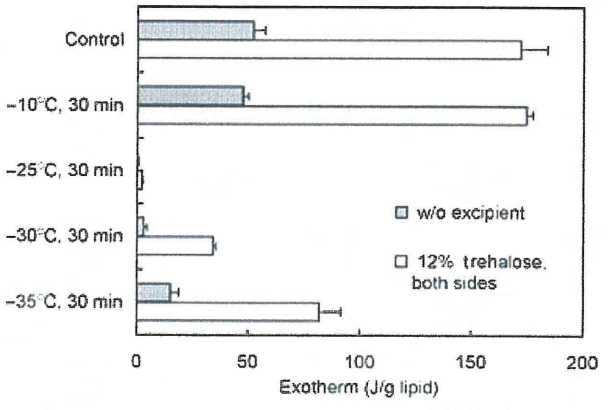

Figure 3. Effect of low temperature holding on internal solution freezing exotherms of DPPC liposome suspensions containing trehalose (0% or 12%, w/w) on both sides of the membrane (10 μL, 4% lipid in Tris–HCl buffer, 0.2 μm). The suspensions were held at different temperatures (−10°C to −35°C) for 30 min during cooling scans at 5°C/min.

DOI 10.1002/jps

exotherm. The absence of apparent osmotic driving force may explain the limited effect of storage at above the bulk solution freezing temperature.

The DPPC liposome suspensions extruded through larger pore size filters (e.g., 0.4 and 0.8 μm) showed larger intraliposomal solution freezing exotherms (Fig. 2a). Factors including the possibility of higher initial solution contents per lipid weight, limited membrane disordering associated with the curvature, and slower dehydration due to the increase in multilamellar membranes would explain the large exotherms. Liposomes composed of phosphatidylcholines of different acyl chain lengths showed retention of the intraliposomal solution down to the homogeneous ice formation temperature in the order of DMPC < DPPC < DSPC (Fig. 2b). The intraliposomal solution freezing exotherm was not observed in the thermal analysis of POPC liposome suspensions (data not shown). All the liposome membranes are below their T_m (POPC: −5°C, DMPC: 24°C, DPPC: 41°C, DSPC: 54°C) at the bulk solution freezing temperature.[35] Possible differences in the membrane fluidity and rigidity would cause the freeze-induced dehydration to vary.

Effect of Trehalose Distribution on Freezing Profiles of Liposome Suspensions

The effects of intra- and extraliposomal trehalose on the freezing behavior of liposome suspensions were studied. The DPPC liposome suspensions containing trehalose on both sides of the membrane showed larger intraliposomal solution peaks that suggest reduced solution loss upon the bulk solution freezing. For example, cooling of the 0.2 μm DPPC suspensions at 10°C/min resulted in exotherms of approximately 80 and 200 J/g lipid, respectively, in the absence and presence of trehalose (Figs. 2 and 4). The addition of trehalose also lowered the peak temperature of the exotherm (approx. 3°C at 12% trehalose, w/w).[18,34] The trehalose-containing liposome lost a larger amount of the internal supercooled solution during the slower cooling of the suspensions. Temporary pausing of the cooling scan suggested a faster loss of the supercooled solution near the bulk solution freezing temperature (−25°C), also in the trehalose-containing liposome suspensions (Fig. 3). The addition of various low-molecular-weight saccharides and polyols to both sides of the lipid membrane increased the freezing exotherm of the intraliposomal solutions, suggesting that slower freeze-induced dehydration occurred due to the colligatively determined osmotic effect (Fig. 5). The limited effect of dextran on the exotherm could be explained by its lower molar concentration and its possible exclusion from the vicinity of the liposomes in the freeze-concentrated nonice phase.[36] The large (0.4 and 0.8 μm) or lower fluidity (DSPC) liposomes retained higher amounts of

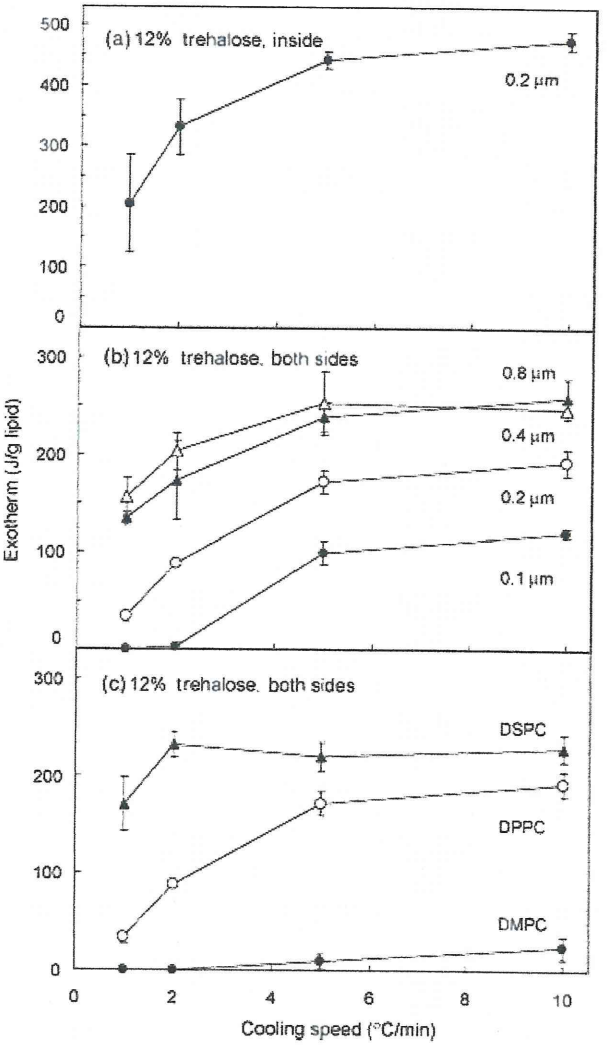

Figure 4. Internal solution freezing exotherms of liposome suspensions containing trehalose (12%, w/w) on (a) the inside and (b, c) both sides of liposomes. Aliquots of suspensions (10 μL, 4% lipid in 10 mM Tris–HCl buffer) containing liposomes with (b) differing extrusion membrane pore sizes (DPPC; 0.1 μm: •, 0.2 μm: ○, 0.4 μm: ▲, and 0.8 μm: △) and (c) lipid compositions (0.2 μm; DMPC: •, DPPC: ○, and DSPC: ▲) were cooled at 1–10°C/min (average ± SD, $n = 3$).

freezable intraliposomal solution in the presence of trehalose on both sides of the membrane (Figs. 4b and 4c).

1,2-Dipalmitoyl-*sn*-glycero-3-phosphocholine liposomes containing trehalose on one side of the membrane showed different freezing behaviors. The addition of higher concentration trehalose to the extraliposomal media reduced the intraliposomal solution freezing exotherm (Fig. 6). The difference in the osmotic pressures across the membrane should induce solution flow that dehydrates the liposomes both prior to cooling and after the bulk solution freezing. The

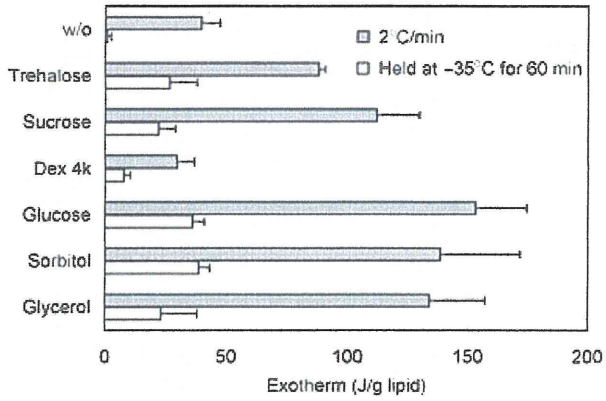

Figure 5. Effect of various extraliposomal solutes (12%, w/w) on internal solution freezing exotherms of DPPC liposome suspensions (10 μL, 4% lipid in 10 mM Tris–HCl buffer, 0.2 μm) obtained via cooling scans at 2°C/min (average ± SD, $n = 3$). Some suspensions were held at −35°C for 60 min during the scan.

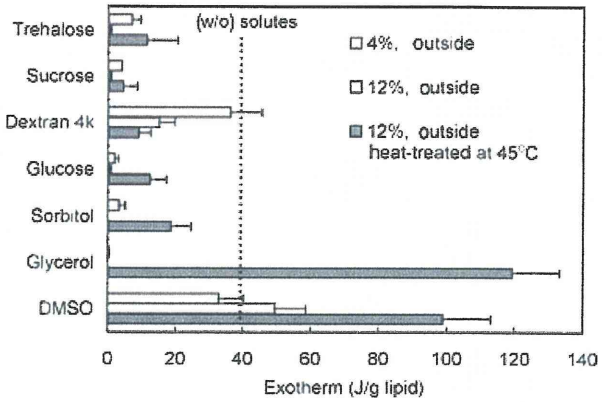

Figure 7. Effect of various extraliposomal solutes (4% and 12%, w/w) on internal solution freezing exotherms of DPPC liposomes obtained via cooling scans of suspensions (10 μL, 4% DPPC in 10 mM Tris–HCl buffer, 0.2 μm) from room temperature to −70°C at 2°C/min. Some suspensions were heat-treated at 45°C for 3 min before the cooling analysis (average ± SD, $n = 3$).

absence of a broad exotherm between the bulk and intraliposomal solution freezing peaks suggested that liposome dehydration before the bulk solution freezing (e.g., osmotic shrinkage) had occurred rather than the freeze-induced dehydration (data not shown).

Other low-molecular-weight saccharides and polyols in the extraliposomal media also reduced the intraliposomal solution freezing exotherms of the DPPC liposomes (Fig. 7). The extraliposomal dextran showed smaller effect to reduce the exotherm compared with the lower-molecular-weight excipients. Prior heat treatment of the liposome suspensions at above T_m of DPPC (45°C, 3 min), apparently increased the intraliposomal solution freezing exotherm of the suspensions containing the externally added glycerol or DMSO. Membrane disordering at and above the transition temperature should allow an influx of the highly permeable small solute molecules, and should, thus, reduce the osmotic effect that dehydrates the liposomes.

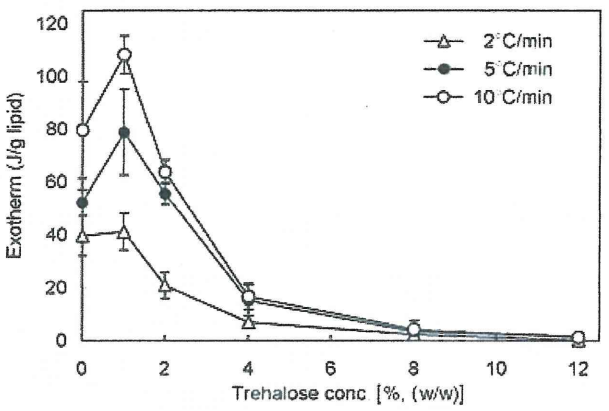

Figure 6. Effect of extraliposomal trehalose (0%–12%, w/w) on internal solution freezing exotherms of DPPC liposome suspensions (10 μL, 4% lipid in 10 mM Tris–HCl buffer, 0.2 μm) obtained by cooling at 2°C/min (△), 5°C/min (•), or 10°C/min (○)(average ± SD, $n = 3$).

The effect of intraliposomal trehalose on the freezing behavior of DPPC liposomes was also studied (Fig. 4a). The suspensions containing trehalose predominantly inside the liposomes showed apparently larger exotherms than those of other suspensions. The absence of the baseline shift at the trehalose transition temperature of maximally freeze-concentrated solutes (T_g') in the heating scan confirmed the low trehalose concentration outside the liposomes (data not shown). Liposomes prepared by extrusion often contain an amount of internal solution that was insufficient to fill the completely spherical structure, which allows inward water flow across the membrane upon exposure of liposomes to lower osmolarity solutions.[37] An increase in the intraliposomal solution content due to osmotic swelling in the initial suspension and limited freeze-induced dehydration can explain the larger ice formation peaks. These results indicated that the osmotic effect made a significant contribution to the freezing behavior of liposomes.

Kinetic stability of the trehalose-containing supercooled intraliposomal solutions was studied to elucidate their relevance in freeze-drying process (Fig. 8). Some liposome suspensions (e.g., trehalose-containing 0.8 μm DPPC liposome) showed small but apparent intraliposomal solution freezing peaks in the scans after a slower cooling (0.5°C/min) followed by being held at −35°C (180 min). The result suggested that some liposomes retain certain amount of internal solutions during freezing segment of pharmaceutical formulation lyophilization usually

DOI 10.1002/jps

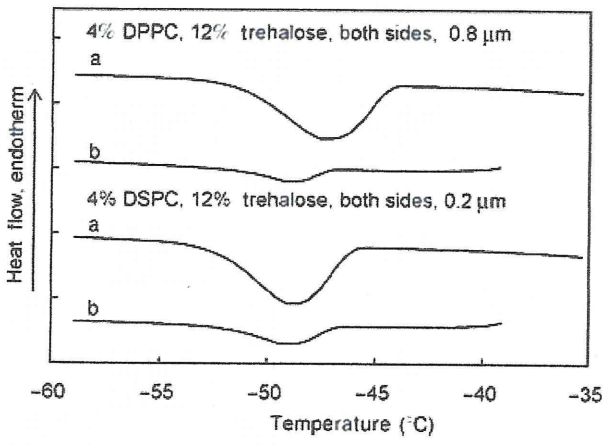

Figure 8. Cooling thermograms of DPPC (0.8 μm) and DSPC (0.2 μm) liposome suspensions containing trehalose (12%, w/w) on both sides of the membrane (10 μL, 4% lipids in 10 mM Tris–HCl buffer). The suspensions were cooled at 5°C/min (a) from room temperature or (b) after slow cooling (0.5°C/min) with a temporary pause at −35°C (180 min).

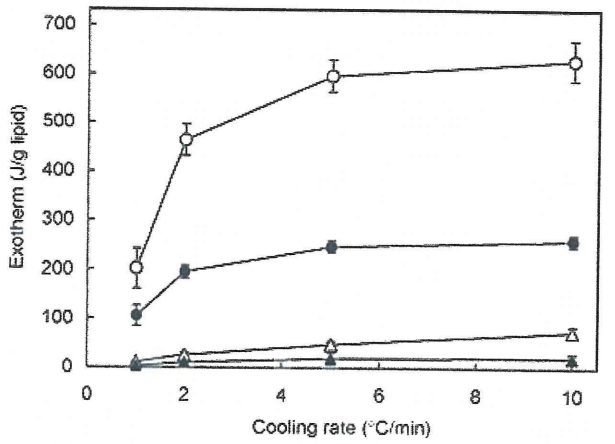

Figure 9. Internal solution freezing exotherms of carboxyfluorescein (25 mM)-containing DPPC liposome suspensions (10 μL, 4% DPPC in 10 mM Tris–HCl buffer, 0.2 μm) without (△) or with 12% trehalose on the outside (▲), inside (○), or both sides (●) of the liposome membrane scanned from room temperature at 1–10°C/min (average ± SD, $n = 3$).

performed via slow cooling (e.g., 0.2–0.5°C/min) down to −35°C to −50°C on the lyophilizer shelf.[38,39] The lower product temperature during the process should lead to freezing of the intraliposomal solutions by the homogeneous ice nucleation mechanism.

Effect of Freeze–Thawing on CF-Encapsulated Liposomes

The relationship between trehalose-induced changes in the liposome freezing behavior and functional stability of liposomes upon freeze–thawing was studied (Figs. 9 and 10). The CF-loaded DPPC liposomes were subjected to thermal analysis and freeze–thawing marker-retention study (a) without trehalose, (b) with trehalose on both sides of the membrane, (c) with trehalose in the intraliposomal solution, or (d) with trehalose in the extraliposomal media. A lower concentration (25 mM; approx. 0.94%, w/w) of CF compared with those in other retention studies (e.g., 100 mM) was used for the experiment to reduce its osmotic effect on the freezing behavior of the liposomes. A thermal transition ($T_g' = -36.2$°C) and absence of other peaks in the heating process of a frozen CF solution (25 mM in Tris–HCl buffer, pH 7.4) indicated that the solute was in a noncrystalline state in the freeze-concentrated phase. The CF-loaded liposome suspensions showed small intraliposomal solution freezing exotherms essentially identical to those of the marker-free samples in the absence of trehalose (Figs. 2 and 9). The liposomes lost a large fraction of the markers upon freeze–thawing of the trehalose-free suspensions cooled down to −35°C (below bulk solution freezing temperature) and −70°C (below intraliposomal solution freezing temperature) at all speeds (Fig. 10).

The DPPC liposomes containing trehalose on both sides of the membrane retained higher intraliposomal solution and encapsulated CF contents under faster cooling (5 and 10°C/min). Small changes of the marker retention in the fast cooling of the suspensions down to −35°C and −70°C suggested that the intraliposomal freezing by itself is not a main cause of the severe marker leakage, at least in the presence of trehalose. A large loss of the intraliposomal solution and

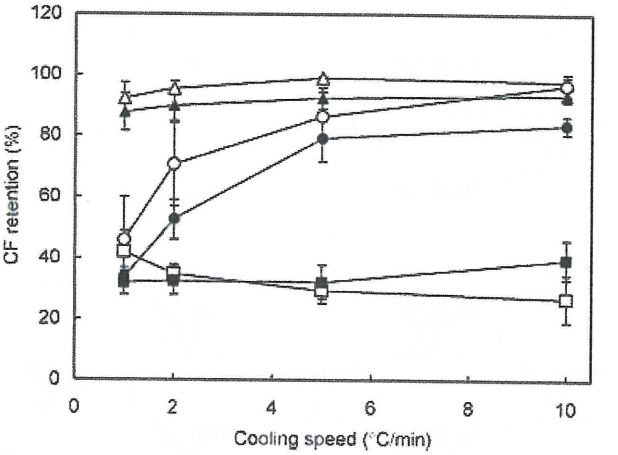

Figure 10. Effect of freeze–thawing on retention of carboxyfluorescein (CF) encapsulated in DPPC liposomes. Aliquots of CF (25 mM)-containing DPPC liposome suspension (10 μL, 4% lipid in 10 mM Tris–HCl buffer, 0.2 μm) without (□, ■) or with 12% trehalose on the outside (△, ▲) or both sides (○, ●) of the liposome membrane were cooled from room temperature to −35°C (open symbols) or −70°C (closed symbols) at 1–10°C/min, and then heated at 10°C/min (average ± SD, $n = 3$).

an accompanying apparent leakage of the marker in the slowly cooled suspensions suggested that membrane damage had occurred that allowed outbound flow of the marker-containing solution during the freezing process. Experiencing the fast-dehydrating temperature range twice in a freeze–thawing cycle should explain the larger change in marker retention compared with that of the intraliposomal freezing exotherm obtained in some cooling procedures. Suspensions containing CF and trehalose only in the intraliposomal solution also showed large intraliposomal solution freezing exotherms (Figs. 4a and 9). Solidification of the suspensions upon freeze–thawing, which hindered the CF retention measurement, confirmed the requirement of trehalose in the extraliposomal media (data not shown).[16]

The externally added trehalose (12%) reduced the CF leakage from the DPPC liposomes upon freeze–thawing at all cooling speeds. The suspensions showed a minor exotherm during the intraliposomal solution freezing. Possible osmotic shrinkage prior to freezing is the likely explanation for the limited internal solution content and the high retention of the encapsulated marker.[4,22,26] The addition of trehalose to the extraliposomal media (12%) induced leakage of less than 1% of the encapsulated CF at room temperature (data not shown).[40] Changes in the color of CF-containing liposome suspensions from yellow to orange by the extraliposomal trehalose suggested an increasing intraliposomal marker concentration due to outbound water flow through membrane diffusion (osmotic shrinkage). The lower intraliposomal solution contents should lead to the limited freeze-induced dehydration and membrane damage. The extraliposomal saccharides should also protect liposomes from membrane injury due to the growing ice surface, an excess concentration of unfavorable solutes (e.g., inorganic salts), and direct contact of concentrated liposome membranes as spacer.[40,39]

Liposome Stabilization by Control of the Osmotic Flow and Internal Freezing

The results indicated varied effect of trehalose on the freezing behavior and functional stability of liposomes upon freeze–thawing depending on its distribution across the membrane. A schematic flow of the liposome freezing behavior is shown in Figure 11. Understanding the physical changes and the encountering stresses should be relevant for strategic stabilization in freeze–thawing and freeze-drying of liposomes. Liposomes prepared by extrusion often do not contain sufficient solutions to fill the spherical structure.[37,41] Exposure of the liposomes either increases (e.g., osmotic swelling in hypotonic media) or decreases (e.g., osmotic shrinkage in hypertonic media) the internal solution content via water diffusion through the membranes. The bulk and intraliposomal solutions freeze at different temperatures, as the processes are initiated by the heterogeneous and homogeneous ice nucleation mechanisms, respectively. The freeze-induced osmotic dehydration and the intraliposomal solution freezing initiated by membrane-penetrating ice crystals should reduce intraliposomal solution content that freeze at the homogeneous ice nucleation temperature.[12,16,34,42] Accordingly, the intraliposomal solution should be in the dehydrated, supercooled, or frozen states in the frozen suspensions depending on the formulation and process factors. The absence of crystallizing solutes (e.g., mannitol) allowed observation of the freeze-induced physical changes through thermal analysis.[28]

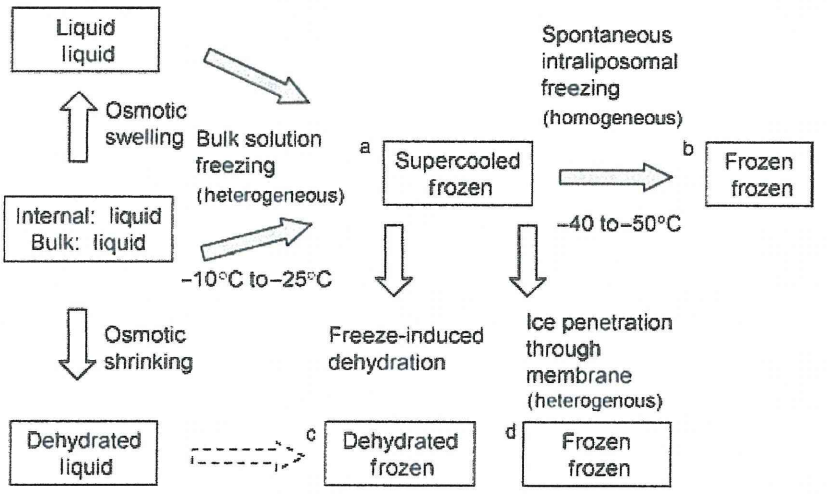

Figure 11. Schematic freezing behaviors of extruded liposome suspensions. The upper and lower rows in each box denote the physical state of the intraliposomal and bulk solutions, respectively. Boxes (a) to (d) indicate suggested physical states of frozen liposome suspensions.

DOI 10.1002/jps

Each step of the freeze-related physical changes induces stresses that affect the stability of liposomes. The growing ice during the bulk and intraliposomal solution freezing should physically damage the liposome membranes. It is possible that the freeze-induced large difference in the osmotic pressure causes larger membrane damage in the DPPC liposomes than in the living cells because of their lower hydraulic permeability, leading to a dehydrating flow of the CF-containing intraliposomal solutions. The liposomes should also experience stresses by ice crystal size growth (Ostwald ripening) and rapid dilution of the surrounding media during the thawing process of the frozen suspensions.[23,43]

The different stability-determining factors during the freezing process of the marker-loaded liposomes from those of the living cells suggest requirement of different strategies for their stabilization.[44] Trehalose protected the marker-loaded liposomes through two types of osmotic effects that prevent the freeze-induced internal solution loss during freeze–thawing. The addition of trehalose to both sides of the liposome membrane prevented both the freeze-induced dehydration and water-soluble marker loss, particularly in the higher cooling rate. The marker retention was also achieved by extraliposomal trehalose that osmotically dehydrates the liposomes through outbound water diffusion without apparent CF release in the initial suspensions. The prior dehydration should prevent the freeze-induced membrane damage even in the slower cooling. These osmotic effects should contribute as one of the major mechanisms by which trehalose protects liposomes during the freezing process besides the water-substitution, bulking, and molecular mobility reduction. The liposomes containing sufficiently high concentrations of cryoprotectants can be vitrified without the apparent ice formation by ultrafast cooling (e.g., immersion of small volume suspensions in liquid nitrogen). The vitrification method would not be practical for large-scale freezing of liposome formulations, although it is a popular way to avoid intracellular freezing during cryopreservation of living cells.[12] Formulation and process optimization of liposome pharmaceuticals should be performed through multiple assay methods (e.g., API retention, liposome fusion, aggregation, and activity of encapsulated enzyme) that appropriately detect the changes caused by different stresses.

The varied physical states of the intraliposomal solutions in the frozen suspensions should directly (e.g., membrane damage due to ice growth) or indirectly (e.g., altered excipient–membrane interactions) affect the liposome stability during freeze-drying process and subsequent storage.[1,5,8,45] The trehalose molecules are required to be distributed in the position spatially accessible to the membrane phospholipids to form the water-substituting interactions that protect the membrane structure from the dehydration stresses. The higher glass transition temperatures (T_g) of the dried solids and resistance against changes by absorbed water should make trehalose a potent stabilizer for lyophilization and subsequent storage of liposomes and biomacromolecules.[39] How the altered freezing behavior affects liposome stability during freeze-drying is an intriguing topic for further study.

The present results indicate the relevance of characterizing the freeze-related physical changes of liposomes for the development of frozen or freeze-dried formulations. The liposome composition and trehalose distribution across the membrane significantly affected the osmotic solution flows that determine the physical states of their intraliposomal solutions and functional stabilities (e.g., CF retention) upon freeze–thawing. Potentially varied molecular interactions between components would also affect liposome stability in the subsequent drying process and in storage. Controlling the osmotically mediated physical changes through formulation design and process optimization would be valuable in the cryopreservation and freeze-drying of liposome pharmaceuticals.

REFERENCES

1. Chen C, Han D, Cai C, Tang X. 2010. An overview of liposome lyophilization and its future potential. J Control Release 142:299–311.
2. Misra A, Jinturkar K, Patel D, Lalani J, Chougule M. 2009. Recent advances in liposomal dry powder formulations: Preparation and evaluation. Expert Opin Drug Deliv 6:71–89.
3. van Winden EC. 2003. Freeze-drying of liposomes: Theory and practice. Methods Enzymol 367:99–110.
4. Wessman P, Edwards K, Mahlin D. 2010. Structural effects caused by spray- and freeze-drying of liposomes and bilayer disks. J Pharm Sci 99:2032–2048.
5. Nakagaki M, Nagase H, Ueda H. 1992. Stabilization of the lamellar structure of phosphatidylcholine by complex formation with trehalose. J Memb Sci 73:173–180.
6. Crowe JH, Crowe LM, Chapman D. 1984. Preservation of membranes in anhydrobiotic organisms: The role of trehalose. Science 223:701–703.
7. Ausborn M, Schreierb H, Brezesinskic G, Fabiand H, Meyere HW, Nuhna P. 1994. The protective effect of free and membrane-bound cryoprotectants during freezing and freeze-drying of liposomes. J Control Release 30:105–116.
8. Crowe JH, Crowe LM, Carpenter JF, Rudolph AS, Wistrom CA, Spargo BJ, Anchordoguy TJ. 1988. Interactions of sugars with membranes. Biochim Biophys Acta 947:367–384.
9. Wolfe J, Bryant G. 1999. Freezing, drying, and/or vitrification of membrane-solute-water systems. Cryobiology 39:103–129.
10. Lovelock JE. 1954. The protective action of neutral solutes against haemolysis by freezing and thawing. Biochem J 56:265–270.
11. Rasmussen DH, Macaulay MN, MacKenzie AP. 1975. Supercooling and nucleation of ice in single cells. Cryobiology 12:328–339.
12. Mazur P. 1984. Freezing of living cells: Mechanisms and implications. Am J Physiol 247:C125–C142.